Econometrics and Statistics 6 (2018) 22–43

Contents lists available at ScienceDirect

Econometrics and Statistics

journal homepage: www.elsevier.com/locate/ecosta

Spot volatility estimation using the Laplace transform

Imma Valentina Curato[a,*], Maria Elvira Mancino[b], Maria Cristina Recchioni[c]

[a] Institute of Mathematical Finance, Ulm University, Helmholtzstrae 18, Ulm 89069, Germany
[b] Department of Economics and Management, University of Florence, Via delle Pandette 32, Florence 50127, Italy
[c] Department of Management, Polytechnical University of Marche, Piazzale Martelli 8, Ancona 60121, Italy

ARTICLE INFO

Article history:
Received 6 January 2016
Revised 31 July 2016
Accepted 31 July 2016
Available online 5 November 2016

JEL Classification:
C14
C58

Keywords:
Laplace transform
Convolution
Spot volatility
Non-parametric estimation
High frequency data
Microstructure noise

ABSTRACT

A new non-parametric estimator of the instantaneous volatility is defined relying on the link between the Laplace transform of the price process and that of the volatility process for Brownian semimartingale models. The proposed estimation method is a global one, in the spirit of methods based on Fourier series decomposition, with a *plus* for improving the precision of the volatility estimates near the boundary of the time interval. Consistency and asymptotic normality of the proposed estimator are proved. A simulation study confirms the theoretical results and Monte Carlo evidence of the favorable performance of the proposed estimator in the presence of microstructure noise effects is presented.

1. Introduction

The Laplace transform has been widely used in the literature on option pricing (see, e.g., Carr and Wu, 2004; Fusai, 2004; Leblanc and Scaillet, 1998; Lee, 2004). More recently, Tauchen and Todorov (2012) introduced the empirical Laplace transform to study the characteristics of the volatility. Nevertheless, the Laplace transform methodology has not been used to estimate the instantaneous volatility. As shown here, a suitable convolution product of the Laplace transform of asset returns is an appropriate tool to build global non-parametric estimators of the instantaneous volatility.

The first steps in the harmonic analysis method to compute instantaneous multivariate volatilities were made by Malliavin and Mancino (2002). A peculiarity of the Fourier estimation procedure is that, in virtue of its own definition, it uses all available observations and avoids any manipulation of the original data (as happens with several alternative proposals which rely on data-synchronization methods), because it is based on the integration rather than differentiation of the time series of prices. Moreover, the Fourier estimation method is a *global method*, unlike methods based on the use of observations in local time windows. This approach allows us to overcome the use of the empirical derivative employed in a vast range of literature to obtain the instantaneous volatility (see the recent book by Ait-Sahalia and Jacod, 2014). A consistent estimator of the spot volatility was defined by Malliavin and Mancino (2009) relying on the finite Fourier transform of the price process over a fixed time interval in the absence of microstructure noise effects. The efficiency of the Fourier method

* Corresponding author.
E-mail address: imma.curato@uni-ulm.de (I.V. Curato).

http://dx.doi.org/10.1016/j.ecosta.2016.07.002

in the presence of microstructure noise has been analyzed and compared with other estimators by Nielsen and Frederiksen (2008) and Mancino and Sanfelici (2008; 2011). The authors show that the Fourier estimator of integrated co-volatilities is substantially unaffected by the presence of microstructure noise contaminations by suitably choosing the number of Fourier coefficients to include in the estimator. More recently, Park et al. (2016) introduce the *Fourier Realized Kernel* estimator and show that it is consistent even in the presence of microstructure noise effects. Limit theorems for the Fourier estimator of integrated multivariate volatility under different sampling schemes are proved by Clement and Gloter (2011), whereas Cuchiero and Teichmann (2013) extend the Fourier method in the presence of jumps.

The Laplace transform method hinges on the same two-step procedure used for the Fourier estimation approach, that is, the convolution product of an integral transform of the asset returns and an inversion formula. Therefore, it presents the same advantage as the Fourier estimation approach with respect to the quadratic variation-based methods, concerning the use of all the available observations without the need for any manipulation of the original data. It also has additional attractive features. From a conceptual point of view, the introduction of the Laplace transform produces two benefits. Firstly, it avoids the artificial "periodization" of the asset price process subjacent to Fourier series methodology, which is responsible for the low precision of the estimate near the boundary of the time interval. Secondly, it leads to the estimator defined in (8), which constitutes a bridge between the two different approaches to compute the volatility, namely, *local* methods based on the quadratic variation formula and the *global* approach via Fourier analysis.

The main analytical result proved here is that under the hypothesis that the price process is a continuous semi-martingale, the Laplace transform of the stochastic volatility function is equal to the Bohr convolution product of the Laplace transform of the price process. Consequently, the transform needs to be inverted to obtain the spot volatility estimator. As a matter of fact, computing the Laplace transform of a given function corresponds to computing the Fourier transform of the function multiplied by a damping exponential factor. Therefore, the Fourier inversion formula is applied to obtain the (damped) volatility function. The proposed estimator considers a long time series of prices by smoothing past data. This procedure generates a spot volatility estimator that employs weighted sums of squared and cross increments of the price process. The quadratic term is like the triangular kernel-based realized estimator studied by Fan and Wang (2008) and Kristensen (2010); however, the convolution product also generates off-diagonal cross products.

We prove that the Laplace estimator of spot volatility is statistically efficient in terms of rate of convergence and asymptotic variance. Under a suitable choice of the relative growth between the number of data, the convolution frequency and the bandwidth, the Laplace estimator has asymptotic variance equal to $(4/3)\sigma^4(t)$ (where $\sigma(t)$ denotes the volatility process) which is the same for the triangular kernel-based realized estimator and the same rate of convergence (see the result by Fan and Wang, 2008). Therefore, we prove that the effect of the cross terms is not detrimental in view of the asymptotic efficiency, if the couple convolution frequency and bandwidth are appropriately selected as indicated in this theory. On the other hand, it is known that the role of the cross terms is crucial for the estimator's robustness in the presence of microstructure noise in the case of the Fourier estimator in Mancino and Sanfelici (2008), the Fourier realized kernel estimator in Park et al. (2016), and the realized kernels in Barndorff-Nielsen et al. (2008). As it concerns the Laplace method, Monte Carlo evidence of their contribution is provided by showing that the Laplace estimator outperforms the triangular kernel-based realized estimator in the presence of microstructure noise both inside the interval of observations and near the boundary.

The finite sample properties of the Laplace estimator are analyzed through an intensive simulation study. The frequency (which appears in the convolution) and the bandwidth (arising in the kernel) must be suitably selected to efficiently implement the estimator. Therefore, a method is proposed to select them in a feasible way by using the realized Laplace transform of volatility introduced by Tauchen and Todorov (2012); numerical evidence that the feasible estimator shows the same performance as the non-feasible one is provided.

The paper is organized as follows. Section 2 contains the main result: the Laplace transform of the volatility function is computed to be the Bohr convolution product of the Laplace transform of the log-price. Given discrete unevenly spaced observations of the price, Section 3 provides the explicit expression of the Laplace estimator with proofs for consistency and asymptotic normality. Section 4 contains the simulation study and Section 5 the conclusions. The proofs are in Appendix A, whereas Appendix B contains some auxiliary lemmas.

The main idea presented here originated during discussions the second author had with Prof. Paul Malliavin when he visited the Scuola Normale Superiore of Pisa in 2004 and it was outlined by Malliavin et al. (2005). We recently decided to further explore this promising idea and, not surprisingly, we found it very interesting. We thus dedicate this work to the memory of Prof. Paul Malliavin with our gratitude.

2. The Laplace transform of volatility

In this section, given a continuous trajectory of the asset price process (continuous semi-martingale model), the Laplace transform of the (latent) volatility process is computed. In fact, this analytical result is key to constructing the spot volatility estimator in the next section.

The evolution of the logarithm asset price process $p(t)$ is described by the stochastic differential equation

$$dp(t) = \sigma(t)dW(t) + b(t)dt, \tag{1}$$

where $W(t)$ is a Brownian motion on a filtered probability space $(\Omega, (\mathbb{F}_t)_{t\in(-\infty,0]}, P)$ satisfying the usual conditions. Further, it is assumed that:

(H.1): the processes $\sigma(t)$ and $b(t)$ are almost surely continuous in $(-\infty, 0]$ and adapted to the filtration $\mathbb{F}$;
(H.2): for any real positive number α,

$$E\left[\int_{-\infty}^{0} e^{\alpha t}\sigma^4(t)\ dt\right] < \infty, \quad E\left[\int_{-\infty}^{0} e^{\alpha t} b^2(t)\ dt\right] < \infty.$$

The choice of the negative half real line as the time horizon is compatible with the fact that a unilateral Laplace transform will be used in the analysis. It is also justified because the proposed estimator is required to smooth past data ($t = -\infty$) with the exponential factor and to retain recent price observations.

The main result of this section is an exact formula relating the Laplace transform of the volatility process to the Laplace transform of the returns. The issue of inverting the Laplace transform in order to reconstruct the volatility process for any time t will be addressed in the next section.

Consider the Laplace transform of the price increment on $(-\infty, 0]$ defined by

$$\mathcal{L}(dp)(z) := \int_{-\infty}^{0} dp(t)\exp(zt). \tag{2}$$

Here, $z = a + \mathrm{i}s$, with $a > 0$ and $\mathrm{i} = \sqrt{-1}$. The existence of (2) is guaranteed by assumptions (H.1) and (H.2).

The following theorem proves that the Laplace transform of the volatility process $\sigma^2(t)$ can be computed exactly through the Bohr convolution product of the Laplace transform (2). The *Bohr convolution product* between two complex functions Φ and Ψ is defined by the limit

$$(\Phi *_B \Psi)(v) := \lim_{R\to+\infty} \frac{1}{2R}\int_{-R}^{R} \Phi(a+\mathrm{i}s)\overline{\Psi}(a+\mathrm{i}(s+v))ds,$$

where $\overline{\psi}$ denotes the conjugate of any complex function ψ.

Theorem 2.1. *Let $\mathcal{L}(dp)$ be defined by (2). Then, under hypotheses (H.1) and (H.2), the following convergence in probability holds for $R \to +\infty$:*

$$\frac{1}{2R}\int_{-R}^{R} \mathcal{L}(dp)(a+\mathrm{i}s)\,\overline{\mathcal{L}(dp)}(a+\mathrm{i}s+\mathrm{i}v)\,ds \to \int_{-\infty}^{0} \sigma^2(t)\exp\big((2a-\mathrm{i}v)t\big)\,dt. \tag{3}$$

The term on the right hand side of (3) is the Laplace transform of the volatility process $\sigma^2(t)$ at $w := 2a - \mathrm{i}v$. Thus, the latent volatility process is meant to be obtained through an inversion formula. More precisely, using the fact that the Laplace transform of a function $f(t)$ is equal to the Fourier transform of the function $f_a(t) := e^{at}f(t)$, for a fixed positive real part, we *invert* the Fourier transform in order to recover the damped volatility process denoted by $\sigma_a^2(t) := e^{2at}\sigma^2(t)$.

Remark 2.2. The statement of Theorem 2.1 follows the same intuition of Theorem 2.1 by Malliavin and Mancino (2009), where the Fourier coefficients of the price process are computed in order to reconstruct the volatility path. However, the use of the Laplace transform has the advantage that it avoids the artificial "periodization" below the Fourier series method, thus improving the accuracy of the volatility trajectory's estimation near the right boundary (i.e., the current time $t = 0$). In fact, given a random function ϕ such that $\phi(0) = \phi(2\pi)$ a.s., the Fourier transform of ϕ is defined on the group of integers $\mathbf{Z}$ by

$$\mathcal{F}(\phi)(k) := \frac{1}{2\pi}\int_0^{2\pi} \phi(t)\ \exp(-\mathrm{i}kt)\,dt.$$

In order to assume that the price process satisfies $p(0) = p(2\pi)$, the process p is eventually modified by Malliavin and Mancino (2009) into the process $\widehat{p}(t) = p(t) - \frac{p(2\pi)-p(0)}{2\pi}t$, which has the same volatility as p. However, from the computational point of view, this periodization procedure affects the boundary behavior of the estimator. Monte Carlo evidence of the different accuracy of the Fourier and the Laplace estimators is given in Section 4.3.

Remark 2.3. Formula (3) depends on an arbitrary positive parameter a. The choice of the parameter a determines the relevance or weight of the past information when very long series of data are used. In fact, by increasing a, the weight of the past information decreases.

3. The Laplace estimator of volatility

In this section a new estimator of spot volatility is proposed, the definition of which is based on the continuous time result stated in Theorem 2.1. Given a discrete, unevenly spaced sampling of the price process $p(t)$, we explain the procedure leading to a consistent estimator of the (damped) instantaneous volatility $\sigma_a^2(t)$ starting from result (3).

Let $(t_{i,n})_{i=0,\dots,k_n}$ be observation times, $-\infty < t_{k_n,n} < \cdots < t_{i+1,n} < t_{i,n} < \cdots < t_{0,n} = 0$. For simplicity, the second index is omitted and we set $k_n = n$. Let ε_t be the Dirac function at point t, and, for any $i \geq 1$, let $\delta_i(p) := -p(t_i) + p(t_{i-1})$. Then

$$dp_n = \sum_{i\geq 1} \delta_i(p)\, \varepsilon_{t_i}$$

and the discrete Laplace transform of price at $z = a + is,\ a > 0$, is given by

$$\mathcal{L}(dp_n)(z) = \sum_{i\geq 1} \delta_i(p) \exp(zt_i). \tag{4}$$

Let the integration interval in (3) be fixed equal to $[-R, R]$, using the identity (see, e.g., the book by Malliavin, 1995)

$$\frac{1}{2R}\int_{-R}^{R} \exp(\mathrm{i}st_i - \mathrm{i}st_j)\, ds = \varphi(R(t_i - t_j)), \tag{5}$$

with $\varphi(\lambda) := \frac{\sin\lambda}{\lambda}$ and the expression (4) of the Laplace transform of dp_n, we find that the left hand side of (3) is equal to

$$\sum_{i,j>0} \delta_i(p)\delta_j(p) \exp(a(t_i + t_j)) \exp(-\mathrm{i}\nu t_j)\varphi(R(t_i - t_j)). \tag{6}$$

Moreover, it can be seen that the right hand side of (3) is equal to

$$\int_{-\infty}^{0} \sigma_a^2(t) \exp(-\mathrm{i}\nu t) dt.$$

Therefore, the inverse Fourier transform of (6) in variable ν must be taken, thus obtaining

$$\sum_{i,j>0} \delta_i(p)\delta_j(p) \exp(a(t_i + t_j))\varphi(R(t_i - t_j)) \frac{1}{2\pi}\int_{-\infty}^{+\infty} \exp(\mathrm{i}\nu(t - t_j)) d\nu. \tag{7}$$

It is advisable to consider a different Fourier inversion formula by weighting the expression in (7) with the kernel $(\frac{\sin\delta\nu}{\delta\nu})^2$, $\delta > 0$. The introduction of a smoothing kernel in the inversion formula is also used efficiently by Park et al. (2016) to define the Fourier realized kernel estimator. Then, we need to compute the Fourier transform of the kernel, that is

$$\frac{1}{2\pi}\int_{-\infty}^{+\infty} \left(\frac{\sin\delta\nu}{\delta\nu}\right)^2 \exp(\mathrm{i}\nu(t - t_j)) d\nu,$$

which produces the triangular function as a localizer.

The previous computation leads to the definition of the following spot volatility estimator, which we will refer to as the *Laplace volatility estimator*:

$$\widehat{\sigma}_a^2[n, R, h](t) := \sum_{i,j>0} \delta_i(p)\delta_j(p)\ \exp(a(t_i + t_j))\varphi(R(t_i - t_j))\, u_h(t - t_j), \tag{8}$$

where $h := 2\delta$, u_h is defined by

$$u_h(t - t_j) := \frac{1}{h}\left(1 - \frac{|t - t_j|}{h}\right)\mathbf{1}_{[-1,1]}\left(\frac{t - t_j}{h}\right) \tag{9}$$

and φ, introduced in (5), is given by

$$\varphi(R(t_i - t_j)) := \frac{\sin(R(t_i - t_j))}{R(t_i - t_j)}. \tag{10}$$

Function (10) is referred to as the modified (rescaled) Dirichlet kernel, because these two kernels are asymptotically equivalent (see, e.g., Barndorff-Nielsen et al., 2008).

Before studying the asymptotic properties of the Laplace estimator some comments are needed. The instantaneous volatility estimator (8) was obtained by combining two arguments: the convolution product of an integral transform of the asset returns and an inversion formula. This two-step procedure is peculiar to harmonic analysis methods such as the Fourier method, and is responsible for the two kernels entering in (8): the modified Dirichlet kernel, which appears as a consequence of the convolution product, and the localizing one, which is the triangular kernel. Thus, the Laplace estimator is expected to have features similar to the Fourier estimator, namely robustness to irregular-asynchronous data observations and the ability to filter out microstructure noise. The first is due to the fact that the estimator incorporates all data through integration, avoiding any preliminary manipulation, while the second is linked to the possibility of cutting the highest frequencies by a suitable choice of the parameter R. However, the latter study, concerning the robustness to microstructure noise, is beyond the scope of the paper.

Finally, we see that the estimator (8) constitutes a bridge between the Fourier global method and estimators based on quadratic variation such as kernel-based spot volatility estimators studied by Fan and Wang (2008), Kristensen (2010) and Mancini et al. (2015) (see also the recent book by Ait-Sahalia and Jacod, 2014 for an updated presentation). In fact, (8) can be written as

$$\sum_i (\delta_i(p))^2 \exp(2at_i)\, u_h(t-t_i) \tag{11}$$

$$+ \sum_{i\neq j} \delta_i(p)\delta_j(p) \exp(a(t_i+t_j))\varphi(R(t_i-t_j))\, u_h(t-t_j), \tag{12}$$

thus identifying a first addend (11), which is a triangular kernel-based realized spot volatility estimator, and a second addend (12) that includes the cross terms. It should be stressed that kernel-based realized estimators only contain the quadratic component like (11), with possibly different kernels. A general result for this latter class of kernel-based spot volatility estimators can be found in the book by Ait-Sahalia and Jacod (2014) (Theorem 8.7 and following remarks therein). On the other hand, in the case of the integrated volatility, the so-called *quadratic estimators* defined by formula (7.3.3) in the book by Ait-Sahalia and Jacod (2014) also consider the contribution of the cross terms. However, the asymptotic normality for the quadratic estimators (i.e., with the cross component) of spot volatility is not known. Further, the presence of the two kernels is peculiar to convolution-based methods such as the Fourier or Laplace methods. In Section 4.3, Monte Carlo evidence is presented for the different behavior of the kernel-based realized estimator with respect to the Laplace estimator and for the relevance of the cross terms to the performance of the estimator in the presence of microstructure noise, through a suitable choice of parameter R.

Finally, it should be emphasized that different choices of the weighting kernel in the inversion formula lead to different formulations of the Laplace-type estimator, in which the triangular kernel is replaced by a different one. This generalization is left to forthcoming research.

3.1. Asymptotic properties

In this section we study the asymptotic properties of the spot volatility estimator defined in (8). The next theorem proves consistency in probability of the Laplace estimator under suitable growth conditions among the mesh of the partition $\rho(n)$, the convolution frequency R, and the bandwidth h. The consistency result is derived under the hypothesis that as $n \to +\infty$ then $t_n \to -\infty$ (*long span*) and $\rho(n) := \max_{i=1,\dots,n} |t_{i-1} - t_i| \to 0$ (*infill*). The interest in studying the long-term asymptotic behavior, even if unusual in the context of the spot volatility, is justified for the purpose of identifying stochastic volatility models. In fact, the drift function is not identified from data observed within a fixed time interval, see also the nonparametric estimators by Bandi and Renò (2010) and Kanaya and Kristensen (2015).

Theorem 3.1. *Let $\widehat{\sigma}^2_a[n,R,h](t)$ be defined as in (8). Suppose that assumptions* (H.1) *and* (H.2) *hold and for all $\alpha > 0$*

$$\sup_{t_n \le t \le 0} E[e^{\alpha t}\sigma^4(t)] < C, \quad \forall\, t_n < 0, \tag{13}$$

where C does not depend on t_n. Then, as $n, R \to \infty$ and $h \to 0$, the following convergence in probability holds:

$$P - \lim \widehat{\sigma}^2_a[n,R,h](t) = \sigma^2_a(t)\,,$$

under the conditions $\rho(n)/h \to 0$ and $R\rho(n) \to c_\rho$, where c_ρ is a positive constant.

Remark 3.2. Condition (13) is not restrictive and is satisfied, for instance, if the variance process follows the CIR model by Cox et al. (1985) or the Vasicek model by Vasicek (1977).

The following theorem proves the pointwise asymptotic normality of the Laplace estimator in the case when the time interval is finite and the partition mesh goes to 0 (infill asymptotic). In this case, it is natural to consider the observation interval to be $[0, T]$ and, for simplicity, $t_i = \frac{iT}{n}$, with $i = 0, \dots, n$. From a mathematical point of view, the damping factor is clearly not needed here. Thus, we consider $a = 0$ in definition (8). The estimator (8) is denoted as $\widehat{\sigma}^2[n,R,h]$ in this case.

Assumptions (H.1) and (H.2) are restated accordingly:

(H.1)′: the processes $\sigma(t)$ and $b(t)$ are almost surely continuous in $[0, T]$,
(H.2)′: $E[\int_0^T \sigma^4(t)\, dt] < \infty, \quad E[\int_0^T b^2(t)\, dt] < \infty$.

We further assume:

(H.3)′: the modulus of continuity of $\sigma(t)$ is $\omega_\sigma(h) = O_p(\sqrt{h|\log(T/h)|})$,
(H.4)′: processes σ and W are independent.

Remark 3.3. Note that (H.2)′ is now implied by (H.1)′. The continuity assumption (H.3)′ is not restrictive as it is satisfied for all common stochastic volatility models. The no-leverage hypothesis (H.4)′, which is often imposed in the related literature (e.g., by Fan and Wang, 2008; Kristensen, 2010; Park et al., 2016), is assumed in order to simplify the proof. Section 4.4 provides Monte Carlo evidence of the behavior of the Laplace estimator with a varying leverage component.

Theorem 3.4. *Suppose that assumptions (H.1)′–(H.3)′–(H.4)′ hold and that $R/n \to c$ as $R, n \to \infty$, where c is a positive constant and $h = O(n^{-\frac{1}{2}}/\log n)$. Then, as $R, n \to \infty$ and $h \to 0$, for any $t \in (0, T)$:*

$$\sqrt{\frac{nh}{T}}\,(\widehat{\sigma}^2[n, R, h](t) - \sigma^2(t)) \to \mathcal{N}\Big(0, \frac{4}{3}(1 + 2\eta(c))\sigma^4(t)\Big),$$

where the stable convergence is in law and the constant $\eta(c)$ is defined in (14).

The constant $\eta(c)$, computed in Lemma B.2, is equal to

$$\eta(c) := \frac{1}{2\tilde{c}^2} r(\tilde{c})(1 - r(\tilde{c})), \tag{14}$$

where $\tilde{c} = c\,\frac{T}{\pi}$ and $r(x) = x - [x]$, with $[x]$ the integer part of x.

Remark 3.5 (Asymptotic variance)**.** Note that $\eta(c)$ defined in (14) is non-negative for any positive c and equal to zero when $c = (\pi/T)k,\ k = 1, 2, \ldots$. Therefore, the smallest value of the asymptotic variance is attained for $c = (\pi/T)k,\ k = 1, 2, \ldots,$ and is equal to $(4/3)\sigma^4(t)$. Non-integer values of $\tilde{c}$ lead to bigger variance. In comparison with classical estimators of spot volatility (see, e.g., Eq. (8.4) p. 262 in the book by Ait-Sahalia and Jacod, 2014) whose asymptotic variance is equal to $2\sigma^4(t)$, the Laplace estimator's asymptotic variance is reduced by a factor 2/3. The precise value of the variance depends on two elements: the constant c, which is the limit of the ratio R/n, and the choice of the two kernels in the definition of the estimator (i.e., the triangular and the modified Dirichlet kernels). In Appendix A by Cuchiero and Teichmann (2013), this variance reduction phenomenon for the Fourier estimator is noted and discussed in terms of a "diversification effect" produced by the fact that the estimator uses the information contained in the whole time series of prices.

It is worth noting that by choosing $T = 2\pi$ (this can always be done by scaling the time variable), we find that the optimal asymptotic variance is obtained for $c = (1/2)k,\ k = 1, 2, \ldots$ and the choice $k = 1$ (i.e., $c = 1/2$) corresponds to the natural choice of the Nyquist frequency for the Fourier estimator. Furthermore, for practical purposes, the number of frequencies is chosen to be less than the number, n, of the available price observations, so that the values $c = 1/2k,\ k = 2, 3, \ldots$ are not effective, while the value $c = 1/2$ is appropriate. These findings suggest the choice $c = \pi/T$ is the natural one in the case of any finite horizon T.

Remark 3.6 (Bandwidth selection)**.** The bandwidth $h = O(n^{-\frac{1}{2}}/\log n)$ is chosen as that of Fan and Wang (2008) and it is related to the modulus of continuity assumption (H.3)′. The exact optimizing constant is difficult to estimate and a method is proposed in Section 4.4. Note that the proof of Theorem 3.4 still holds if it is assumed that $h = O(n^{-\beta})$, for $\beta > \frac{1}{2}$, thus implying a rate of convergence equal to $\frac{1}{2}(1 - \beta) < \frac{1}{4}$.

As a consequence of Remarks 3.5 and 3.6, with these choices for the bandwidth h and frequency R, the Laplace estimator has the same rate of convergence and asymptotic variance as the triangular kernel-based realized estimator defined by (11) obtained by Fan and Wang (2008). In particular, it is proved that the effect of adding the cross term (12) is not detrimental in view of the asymptotic efficiency with an appropriate choice of c (in other words, R/n). Moreover, Section 4 presents Monte Carlo evidence suggesting that the cross terms (12) play a relevant role in order to preserve the performance of the Laplace estimator when the data are contaminated by microstructure noise effects. In this case, we see that the choice $R/n \to 0$ is preferable.

Remark 3.7. The constant $\eta(c)$ also appears in the asymptotic variance of the Fourier estimator of integrated volatility computed by Clement and Gloter (2011). This is not surprising since the rescaled Dirichlet kernel and the kernel φ in (5) are asymptotically equivalent.

4. Simulation study

In this section the finite sample properties of the Laplace estimator are investigated. Firstly, the asymptotic normality of the Laplace estimator is analyzed, along with its behavior with respect to the sampling rate. The study is also conducted using a model with varying leverage dependence. The performance of the Laplace estimator is then compared to that of the Fourier and triangular kernel-based realized estimators in a more realistic Monte Carlo experiment where prices are contaminated with microstructure noise effects.

The main finding that emerges from the Monte Carlo analysis is that the Laplace estimator improves the boundary accuracy while maintaining good performance in the presence of microstructure noise contaminations. Namely, it joins the features of a *local* estimator (like the triangular kernel-based realized estimator) to those of a *global* estimator (like the Fourier estimator), thus acting as a bridge between these two classes of estimators.

Table 1
Laplace estimator versus sampling rate.

Sampling rate	*IMSE*	*IBIAS*	$MSE(T_b)$	$BIAS(T_b)$
1 s	1.96e−4	−1.06e−4	2.29e−4	4.18e−4
5 s	5.79e−4	−2.06e−3	6.63e−4	−1.57e−3
10 s	1.07e−3	−4.68e−4	1.14e−3	4.71e−3
20 s	2.05e−3	−1.94e−3	2.05e−3	−9.39e−4
60 s	6.08e−3	−2.39e−3	6.07e−3	−1.44e−3

4.1. Monte Carlo data-set and error measures

We consider the following stochastic volatility model:

$$dp(t) = \sigma(t)dW(t),$$
$$d\sigma^2(t) = \gamma\,(\theta - \sigma^2(t))dt + \nu\sigma(t)\,dZ(t),$$

where $W(t)$, $Z(t)$ are standard Brownian motions such that $\langle dW, dZ\rangle_t = \lambda\,dt$. The model parameters are chosen as those by Bandi and Russell (2006) and Mancino and Sanfelici (2008), that is, $\gamma = 0.01$, $\theta = 1$, $\nu = 0.05$, $\sigma_0^2 = 1$, and $p_0 = \log(100)$. Moreover, five values of λ are considered: $\lambda = -1, -0.5, 0, 0.5, 1$. It is worth noting that for $\lambda = 0$, this model is the zero-drift stochastic volatility model used by Kristensen (2010) to study the performance of some kernel based spot volatility estimators. By using the explicit Euler discretization scheme, each value of the correlation coefficient, λ, is used to compute second-by-second return and variance paths over a daily trading period of $T = 6$ h $= 6/24$ days for a total of 504 trading days (about two years) with $n = 21,600$ observations per day.

In the proposed experiments, the performance of the considered estimator $\widehat{\sigma}^2(t)$ is measured near the boundary, numerically evaluating the mean squared error

$$MSE(t) = E[(\widehat{\sigma}^2(t) - \sigma^2(t))^2]$$

and the bias

$$BIAS(t) = E[\widehat{\sigma}^2(t) - \sigma^2(t)]$$

at $t = T_b = T - \epsilon$. In addition, the performance over the interval $[T_1, T_2] \subset [0, T]$ is assessed by using the integrated mean squared error

$$IMSE = \frac{1}{T_2 - T_1}\int_{T_1}^{T_2} MSE(t)dt$$

and the integrated bias

$$IBIAS = \frac{1}{T_2 - T_1}\int_{T_1}^{T_2} BIAS(t)dt\,.$$

Thereafter, $\epsilon = 0.001$, $T_b = 0.2499$, $T_1 = 0.01136$, and $T_2 = 0.23864$.

4.2. Finite sample properties

In this section we investigate the asymptotic normality of the Laplace estimator and its behavior with respect to the sampling rate and the leverage parameter.

First, the results of Theorem 3.4 are illustrated using the simulated trajectories of 1-second returns with $\lambda = 0$ as described in Section 4.1. The bandwidths R and h are chosen according with Remarks 3.5 and 3.6, that is, $R = (\tilde{c}\pi/T)(n+1)$ (where $\tilde{c}$ appears in (14)) and $h = 16(\pi/T)/(\sqrt{n}\log n)$. The constant $16(\pi/T)$ is obtained according to the method explained in Section 4.4. For $n = 21600$, Fig. 1 shows the empirical distributions of $\sqrt{nh/T}(\widehat{\sigma}^2(t) - \sigma^2(t))/\sigma^2(t)$, $t = 0.2228$, with $\tilde{c} = 1$ (Fig. 1 (a)), $\tilde{c} = 4$ (Fig. 1 (b)), $\tilde{c} = 1/2$ (Fig. 1 (c)), $\tilde{c} = 1/4$ (Fig. 1 (d)) and the corresponding distributions $\mathcal{N}\big(0, \frac{4}{3}(1 + 2\eta(c))\big)$. The empirical distributions shown in Fig. 1 confirm the results of Theorem 3.4. In fact, when $\tilde{c} = 1$ and 4 (i.e., integer values), the variance attains its smallest value (i.e., 4/3), while the variance increases when $\tilde{c} = 1/2$ and 1/4. A single sample Kolmogorov–Smirnov (KS) goodness-of-fit hypothesis test is used. The quantity H shown in Fig. 1 is equal to zero when the null hypothesis is not rejected and equal to one when this hypothesis is rejected at significance level 0.05 (i.e., 5%). The figure also shows the corresponding "P-value" of the KS test.

The second experiment shows the behavior of the Laplace estimator with respect to the sampling rate $\rho(n)$. This experiment uses a dataset with different sampling specifications while $\lambda = 0$. Five sampling rates are considered: 1 s, 5 s, 10 s, 20 s, and 1 min. For each choice of the sampling rate, the bandwidths $R = (\pi/T)(n+1)$, $h = 16(\pi/T)/(\sqrt{n}\log n)$ are used. From left to right, Table 1 shows the sampling rate, the integrated mean squared error, *IMSE*, the integrated bias, *IBIAS*, the mean squared error $MSE(T_b)$ and the bias $BIAS(T_b)$.

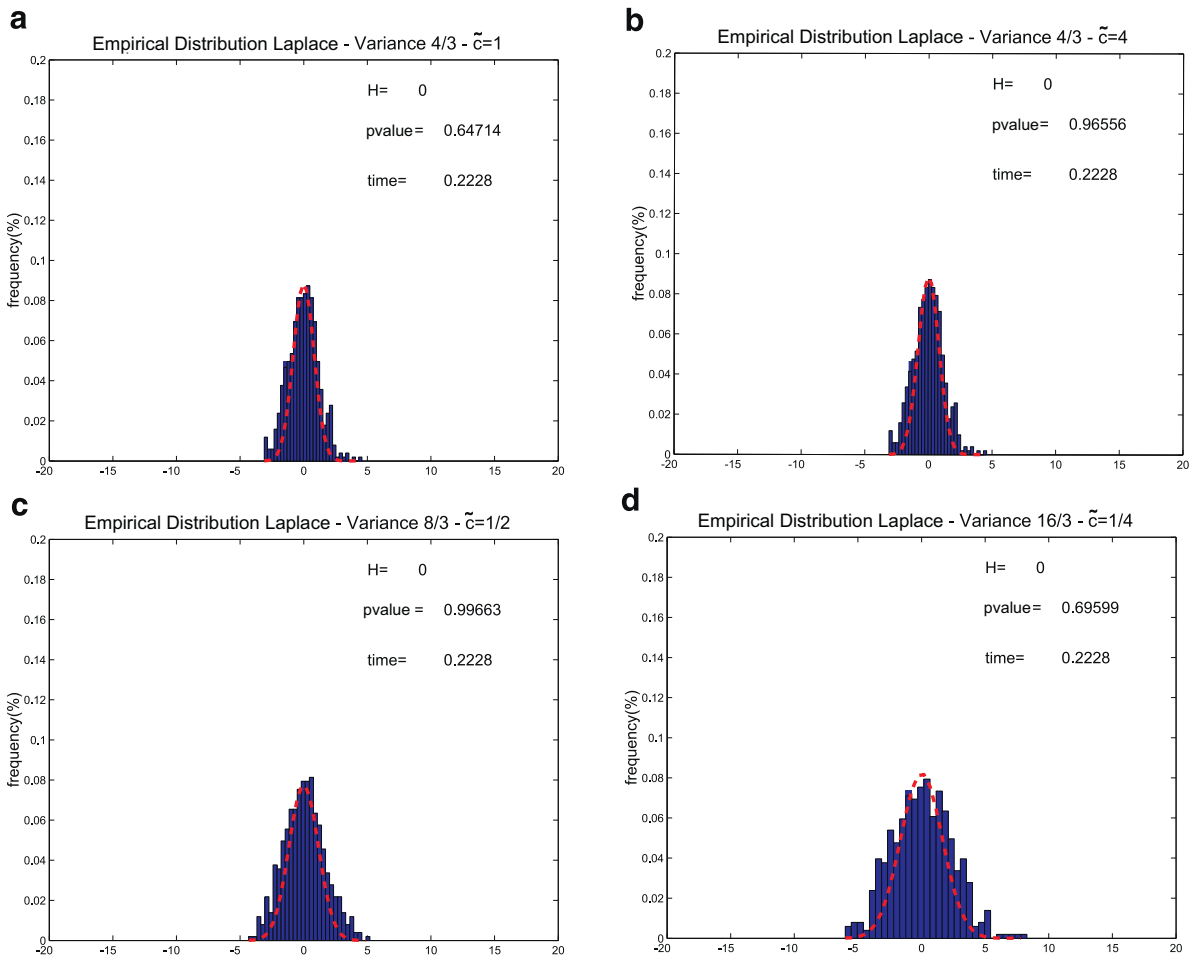

Fig. 1. Empirical distribution of $\sqrt{nh/T}(\hat{\sigma}^2(t) - \sigma^2(t))/\sigma^2(t)$ for different values of $\tilde{c}$, $\tilde{c} = 1$ (a), 4 (b), 1/2 (c), 1/4 (d).

Table 2
Laplace estimator with leverage effects, sampling rate 1 s.

λ	*IMSE*	*IBIAS*	$MSE(T_b)$	$BIAS(T_b)$
−1	2.05e−4	3.02e−3	2.46e−4	−1.56e−2
−0.5	2.47e−4	3.83e−3	2.15e−4	−1.46e−2
0	1.96e−4	−1.06e−4	2.29e−4	4.18e−4
0.5	2.75e−4	4.87e−3	1.44e−4	−1.20e−2
1	2.28e−4	4.89e−3	1.19e−4	−1.09e−2

We conclude this section with a study of the Laplace estimator's behavior with respect to the leverage parameter, λ, $\lambda = -1, -0.5, 0.0, 0.5, 1$. Table 2 shows the results of this experiment in the same format as Table 1. It can be seen that the MSE does not deteriorate when $\lambda \neq 0$, suggesting that the method could be employed in a model with leverage effects.

4.3. Comparison with related estimators

The Monte Carlo experiment conducted in this section aims to study the performance of the Laplace estimator in a more realistic scenario presenting market microstructure noise effects in comparison with the performance of two alternative estimators of spot volatility: the Fourier estimator and the triangular kernel-based realized estimator. These estimators were selected because they are closely related to the Laplace estimator, even if from different perspectives. First, the Fourier and Laplace estimators are both defined based on the Bohr convolution of the corresponding transforms. On the other hand, the triangular kernel-based realized estimator is the *diagonal term* of the Laplace one, as stressed in the decomposition by (11) and (12), and it belongs to the class of realized-type spot volatility estimators.

For the reader's convenience we recall the definition of these estimators. The Fourier estimator of the spot volatility is defined for any $t \in [0, T]$:

$$\widehat{\sigma}^2_{FR}(t) := \sum_{|k|<M} \left(1 - \frac{|k|}{M}\right) c_k(\sigma^2_{n,N}) e^{\mathrm{i}\, k\, (2\pi/T)t}, \tag{15}$$

where $c_k(\sigma^2_{n,N})$ is defined for any $|k| \leq M$ by

$$c_k(\sigma^2_{n,N}) := \frac{T}{2N+1} \sum_{|s|\leq N} c_s(dp_n)\, c_{k-s}(dp_n), \tag{16}$$

and, for any $|k| \leq 2M$,

$$c_k(dp_n) := \frac{1}{T} \sum_{i=0}^{n-1} e^{\mathrm{i}\, k\, (2\pi/T)t_i} \delta_i(p), \tag{17}$$

where $\delta_i(p) := p(t_{i+1}) - p(t_i),\ i = 0, 1, \ldots, n-1$. An elementary computation and formulae (15)–(17) show that parameter M^{-1} acts as the bandwidth h and N controls the number of the Fourier price coefficients included in the Bohr convolution product, as done by the parameter R in the Laplace estimator. The cutting frequency N must be chosen to be less than or equal to the Nyquist frequency, $n/2$, in order to avoid aliasing effects, as explained by Mancino and Recchioni (2015).

The triangular kernel-based realized estimator can be expressed as

$$\widehat{\sigma}^2_{TR}(t) = \sum_{i=0}^{n-1} u_h(t - t_i)(\delta_i(p))^2,$$

where the kernel u_h is given by (9).

The Laplace, Fourier, and triangular kernel-based realized estimators are rescaled by the quantity $\sum_{i=0}^{n-1} K(t - t_i)(t_{i+1} - t_i)$, where K is the triangular kernel in the case of the Laplace and triangular kernel-based realized estimator and the Fejér kernel in the case of the Fourier estimator. This scaling does not change the asymptotic properties of the estimators but it improves their performance (see also Kristensen, 2010; Mancini et al., 2015).

We assume that the logarithms of the observed prices $\widetilde{p}(t_i)$ are given by

$$\widetilde{p}(t_i) = p(t_i) + \eta(t_i), \quad i = 0, \ldots, n,$$

where p is the efficient log-price process defined by (1) and η describes the microstructure noise component, which is assumed to have an MA(1) structure with a negative first-order autocorrelation. More precisely:

(M.I) the random shocks $\eta(t_i)$ for any $i = 0, 1, \ldots, n$ are independent and identically distributed with the Gaussian distribution $\mathcal{N}(0, \widetilde{\eta}^2)$;
(M.II) the true return process $\delta_i(p)$ is independent of $\eta(t_i)$ for any $i = 1, \ldots, n$ and for any n.

We choose $\widetilde{\eta} = \xi\, std(r)$, where $std(r)$ is the standard deviation of the 1-second returns. The quantity ξ is the so called noise-to-signal ratio (see Barndorff-Nielsen et al., 2009 for further details).

The following experiment examines the performance of the Laplace, Fourier, and triangular kernel realized estimators of the spot volatility over the interval $[T_1, T_2] \subset [0, T]$ and near the boundary (i.e., $t = T_b$) using high frequency data, both in the absence ($\xi = 0$) and in the presence ($\xi \neq 0$) of market microstructure noise effects. Five values of the noise-to-signal ratio are considered: $\xi = 0$ (no noise), 0.4, 0.8, 1.6, 3.2.

The bandwidths must be selected for each value of ξ and each estimator. This selection is made in the absence of noise as in Section 4.2 for the Laplace estimator (i.e., $R = (\pi/T)(n+1)$, $h = 16(\pi/T)/(n^{1/2}\log n)$), as suggested by Mancino and Recchioni (2015) for the Fourier estimator (i.e., $N = n/2$, $M^{-1} = 16\pi/(n^{1/2}\log n)$), and as suggested by Fan and Wang (2008) for the triangular kernel-based realized estimator (i.e., $h = 16(\pi/T)/(n^{1/2}\log n)$). In order to make the comparison among the cited estimators easier in the case of noise, R and h are parameterized as follows:

$$R = c_R(n^\alpha + 1), \qquad h = \frac{c_h}{n^\beta}, \qquad \alpha,\ \beta > 0, \tag{18}$$

where the exponents α and β may assume five values, namely 1/8, 1/4, 1/3, 1/2, 2/3, 1, while $c_R = \pi/T$ and $c_h = 16(\pi/T)$. The values of h and R in the form (18) are determined by unfeasible minimization of the (simulated) integrated mean squared error and by unfeasible minimization of the (simulated) mean squared error at the boundary of the interval, as explained in Section 4.2. Note that in the case of the triangular kernel-based estimator, only the bandwidth h must be chosen.

The first line of the three panels in Table 3 shows the performance of the three estimators when used to estimate the volatility with the high frequency data not affected by noise in terms of the integrated mean squared error, *IMSE*, the integrated bias, *IBIAS*, the mean squared error, $MSE(T_b)$, and the bias, $BIAS(T_b)$. These lines show that the estimators have similar performance within the time interval, while the accuracy of the Fourier estimator deteriorates on the boundary. The Laplace estimator matches the good performance of the kernel estimator at the boundary. From left to right, the subsequent lines

Table 3
Laplace, Fourier, and triangular kernel realized estimators in the absence of noise and under noise specification (M.I)–(M.II).

Laplace estimator						
Noise-to-signal ratio ξ	(α^i, β^i)	*IMSE*	*IBIAS*	(α^b, β^b)	$MSE(T_b)$	$BIAS(T_b)$
0.0		1.96e−4	−1.06e−4		2.29e−4	4.18e−4
0.4	$(\frac{2}{3}, \frac{1}{2})$	2.85e−3	1.46e−3	$(\frac{2}{3}, \frac{1}{2})$	2.94e−3	2.74e−3
0.8	$(\frac{2}{3}, \frac{1}{2})$	2.86e−3	3.54e−3	$(\frac{2}{3}, \frac{1}{2})$	2.94e−3	4.82e−3
1.6	$(\frac{2}{3}, \frac{1}{2})$	3.01e−3	1.18e−2	$(\frac{2}{3}, \frac{1}{2})$	3.11e−3	1.31e−2
3.2	$(\frac{2}{3}, \frac{1}{2})$	5.04e−3	4.51e−2	$(\frac{2}{3}, \frac{1}{2})$	5.21e−3	4.64e−2
Fourier estimator						
Noise-to-signal ratio ξ	(α^i, β^i)	*IMSE*	*IBIAS*	(α^b, β^b)	$MSE(T_b)$	$BIAS(T_b)$
0.0		1.43e−4	−1.56e−3		1.49e−2	−3.86e−2
0.4	$(\frac{2}{3}, \frac{2}{3})$	4.81e−3	7.83e−4	$(1, \frac{2}{3})$	1.58e−1	3.76e−1
0.8	$(\frac{2}{3}, \frac{2}{3})$	4.84e−3	2.91e−3	$(\frac{2}{3}, \frac{2}{3})$	5.68e−1	6.36e−2
1.6	$(\frac{2}{3}, \frac{2}{3})$	3.22e−3	1.15e−2	$(\frac{2}{3}, \frac{2}{3})$	1.09	1.78e−1
3.2	$(\frac{2}{3}, \frac{1}{2})$	1.63e−2	8.12e−3	$(\frac{2}{3}, \frac{2}{3})$	1.19	4.97e−1
Triangular kernel realized estimator						
Noise-to-signal ratio ξ	β^i	*IMSE*	*IBIAS*	β^b	$MSE(T_b)$	$BIAS(T_b)$
0.0		1.68e−4	−1.42e−4		2.14e−4	9.31e−4
0.4	$\frac{2}{3}$	1.02e−1	3.19e−1	$\frac{2}{3}$	1.03e−1	3.21e−1
0.8	$\frac{2}{3}$	1.63	1.27	$\frac{2}{3}$	1.64	1.27
1.6	$\frac{2}{3}$	26.25	5.12	$\frac{2}{3}$	26.14	5.11
3.2	$\frac{1}{2}$	418.4	20.45	$\frac{1}{2}$	418.2	20.43

of Table 3 show, for the Laplace and Fourier estimators (respectively the triangular kernel-type estimator), the optimal pair (α^i, β^i) (respectively the optimal value β^i), the integrated mean squared error, *IMSE*, the integrated bias, *IBIAS*, the optimal pair (α^b, β^b) (respectively the optimal value β^b), the mean squared error, $MSE(T_b)$, and the bias, $BIAS(T_b)$. Table 3 provides numerical evidence that the Fourier and Laplace estimators have a good performance over the interval $[T_1, T_2] \subset [0, T]$ and outperform the triangular kernel-type estimator in the presence of microstructure noise effects.

A comment is now due regarding the optimal bandwidths (α^i, β^i) and (α^b, β^b) shown in Table 3. As observed by Mancino and Sanfelici (2008) for the Fourier estimator of integrated volatility, cutting the highest frequencies in the Fourier estimator of spot volatility permits the high-frequency noise components to be filtered out, providing very accurate volatility estimates over the interval. More specifically, the optimal value of α^i goes from 1 to 2/3 in the presence of noise. The parameter β^i, which is related to M through $M = [n^{\beta^i}/c_h]$, is equal to 2/3 if $\xi \leq 1.6$ and to 1/2 if $\xi > 1.6$. The optimal pairs (α^b, β^b) relative to the Fourier estimator are not really significant since the estimator loses accuracy near the boundary. The Laplace estimator cuts the highest frequencies as the Fourier estimator and (α^i, β^i) is always equal to (α^b, β^b). This suggests that bandwidths α^i and β^i determined by minimizing the integrated mean squared error perform well even near the boundary of the time interval.

4.4. Empirical bandwidth selection

In the previous Monte Carlo studies, the bandwidth selection for the Laplace estimator of spot volatility was made following Remarks 3.5 and 3.6 in the absence of microstructure noise effects and through an unfeasible minimization of the (simulated) integrated mean squared error in the presence of microstructure noise.

In this section we repeat the experiment of Section 4.3 using a feasible bandwidth selection method that employs the estimator of the realized Laplace transform of volatility introduced by Tauchen and Todorov (2012), which is defined as follows:

$$V_T(u) := \frac{1}{T}\sum_{i=1}^{n} \rho(n) \cos\left(\sqrt{2u}\frac{\delta_i(p)}{\sqrt{\rho(n)}}\right), \ u \in [0, +\infty).$$

In the absence of noise, this is a consistent estimator of:

$$L_T(u) := \frac{1}{T}\int_0^T e^{-u\sigma^2(s)} ds. \tag{19}$$

Therefore, given the Laplace estimator of spot volatility (8) where the frequency $R = (\pi/T)(n+1)$ is chosen according to Remark 3.5 and the bandwidth h has the form $h = b(\pi/T)/(n^{1/2}\log n)$, the unknown constant b can be determined by

Table 4
Optimal pair $(\alpha_*^{RLT}, \beta_*^{RLT})$ obtained using the realized Laplace transform of volatility with microstructure noise specification (*M.I*)–(*M.II*) and the filtered signal.

ξ	$(\alpha_*^{RLT}, \beta_*^{RLT})$	D_{RLT}^*	$BIAS_{RLT}^*$	*IMSE*	*IBIAS*
0.4	$(\frac{2}{3}, \frac{1}{2})$	1.29e−3	2.73e−1	2.85e−3	1.46e−3
0.8	$(\frac{2}{3}, \frac{1}{2})$	1.26e−3	1.72e−2	2.86e−3	3.54e−3
1.6	$(\frac{2}{3}, \frac{1}{2})$	1.21e−3	1.66e−2	3.01e−3	1.18e−2
3.2	$(\frac{2}{3}, \frac{1}{2})$	9.86e−4	1.44e−2	5.04e−3	4.51e−2

minimizing

$$D_{RLT} = \int_0^{u_{max}} E[(V_T(u) - \widehat{L}_T(u))^2]du\,, \tag{20}$$

where u_{max} is a conveniently chosen positive constant and $\widehat{L}_T$ is given by

$$\widehat{L}_T(u) := \frac{1}{T}\int_0^T e^{-u\,\tilde{\sigma}^2(s)}ds\,. \tag{21}$$

That is, the unknown volatility in (19) is replaced with the Laplace estimated volatility. Note that D_{RLT} is not the integrated mean squared error of the estimator of the empirical Laplace transform since $\widehat{L}_T$ is used instead of L_T in formula (20). However, minimizing D_{RLT} is an efficient way to select b in the absence of microstructure noise effects since V_T is a consistent estimator of L_T in the absence of noise. The choice of $b \approx 16$ comes from the numerical minimization of (20), approximating the integrals appearing in (20) and (21) with composite rectangular quadrature rule, where $u_{max} = 4$, the sampling rate of the log-price equals 1 sec, and the sampling rate of the estimated volatility equals 10 s.

In the presence of microstructure noise, the previous approach cannot be applied directly since the estimator V_T is not robust to noise, as partially addressed by Tauchen and Todorov (2012). Therefore, V_T^* is defined to be

$$V_T^*(u) := \frac{1}{T}\sum_{i=1}^{n}\rho(n)\left(\sqrt{2u}\frac{\delta_i(p^*)}{\sqrt{\rho(n)}}\right),$$

where the returns $\delta_i(p^*)$, $i = 1, 2, \ldots, n$, are obtained from the noisy returns, $\delta_i(\widetilde{p})$, $i = 1, 2, \ldots, n$, by applying a signal smoothing technique which uses the Fourier transform algorithm and cuts frequencies higher than the Nyquist frequency. We select R and h among the values (18) by minimizing the following quantity:

$$D_{RLT}^* = \int_0^{u_{max}} E[(V_T^*(u) - \widehat{L}_T(u))^2]du.$$

The results obtained are shown in Table 4. The first four columns of the table show, respectively, the noise-to-signal ratio ξ, the pair $(\alpha_*^{RLT}, \beta_*^{RLT})$ of exponents α, β used to parameterize R and h in the form (18) (which minimize D_{RLT}^*), the minimum value of D_{RLT}^*, and the corresponding bias $BIAS_{RLT}^*$. The last two columns show the (simulated) integrated mean squared error, *IMSE*, and the (simulated) integrated bias, *IBIAS*, obtained using the values of R and h corresponding to the optimal pair $(\alpha_*^{RLT}, \beta_*^{RLT})$. Table 4 shows that the combined use of a simple filtering technique and the estimator of the realized Laplace transform allows the values of R and h to be selected to provide satisfactory estimates of the spot volatility. In fact, the bandwidth selection made by minimizing D_{RLT}^* and the selection using the (simulated) integrated mean squared error in Section 4.3 provide the same results.

5. Conclusions

We have proposed a non-parametric estimator of spot volatility based on the Bohr convolution of the log-price Laplace transform and proved its consistency and asymptotic normality. While this estimator belongs to the class of estimators based on suitable integral transforms and inversion formulas like the Fourier estimator proposed by Malliavin and Mancino (2002), it substantially improves the accuracy of the latter near the boundary of the time interval. In addition, the Monte Carlo study shows numerical evidence that the Laplace estimator is capable of filtering out microstructure noise effects by carefully selecting the frequency/bandwidth pair R, h. This finding makes the Laplace estimator easy to implement and accurate when dealing with high-frequency financial data. Therefore, the development of spot volatility estimators based on the convolution of suitable transforms of the log-price as well as the statistical properties of the Laplace estimator in the presence of noise deserves further investigation.

Acknowledgments

The authors wish to thank the Editor and two anonymous reviewers for helpful comments which led to a significant improvement of the paper.

Appendix A. Proofs

In what follows, C denotes a constant, which is not necessarily always the same.

Firstly, it is shown that the drift component $b(t)$ of the semimartingale $p(t)$ makes no contribution to formula (3).

Lemma A.1. *Let $p^m(t)$ be the martingale part of the price process $p(t)$, that is, let $dp^m(t) = \sigma(t)dW(t)$. Then, it almost surely holds that*

$$\mathcal{L}(dp) *_B \mathcal{L}(dp) = \mathcal{L}(dp^m) *_B \mathcal{L}(dp^m). \tag{22}$$

Proof. Observe that $p^m(t)$ has the same volatility function of the process $p(t)$ and that

$$\mathcal{L}(dp)(s) = \mathcal{L}(dp^m)(s) + \mathcal{L}(b)(s).$$

We prove that the three convolutions $\mathcal{L}(b) *_B \mathcal{L}(dp^m)$, $\mathcal{L}(dp^m) *_B \mathcal{L}(b)$ and $\mathcal{L}(b) *_B \mathcal{L}(b)$ give a.s. zero contribution. Therefore, (22) holds a.s. Firstly, we show that a.s. $\mathcal{L}(b) *_B \mathcal{L}(b) = 0$. For any $v \in \mathbb{R}$, consider

$$(\mathcal{L}(b) *_B \mathcal{L}(b))(v) = \lim_{R\to+\infty} \frac{1}{2R} \int_{-R}^{R} \mathcal{L}(b)(a+is)\overline{\mathcal{L}(b)}(a+is+iv)ds. \tag{23}$$

Using the Cauchy–Schwartz inequality,

$$\frac{1}{2R} \int_{-R}^{R} \mathcal{L}(b)(a+is)\overline{\mathcal{L}(b)}(a+is+iv)ds \le \left(\frac{1}{2R} \int_{-R}^{R} |\mathcal{L}(b)(a+is)|^2 ds\right)^{\frac{1}{2}} \left(\frac{1}{2R} \int_{-R}^{R} |\overline{\mathcal{L}(b)}(a+is+iv)|^2 ds\right)^{\frac{1}{2}}. \tag{24}$$

With the Plancherel equality we obtain

$$\int_{-\infty}^{+\infty} |\mathcal{L}(b)(a+is)|^2 ds = \int_{-\infty}^{+\infty} |\mathcal{F}(\widetilde{b}_a)(s)|^2 ds = \int_{-\infty}^{+\infty} (\widetilde{b}_a(s))^2 ds,$$

where $\widetilde{b}_a(t) = \mathbf{1}_{(-\infty,0]}(t)e^{at}b(t)$ and $\mathcal{F}(\widetilde{b}_a)(s) = \int_{-\infty}^{+\infty} e^{ist}\widetilde{b}_a(t)dt$. It thus follows that:

$$\limsup_{R\to\infty} \frac{1}{2R} \int_{-R}^{R} |\mathcal{L}(b)(a+is)|^2 ds = 0.$$

Finally, using (23) and (24),

$$\|\mathcal{L}(b) *_B \mathcal{L}(b)\|_{L^\infty} = 0.$$

The same argument proves that the terms $\mathcal{L}(b) *_B \mathcal{L}(dp^m)$ and $\mathcal{L}(dp^m) *_B \mathcal{L}(b)$ give zero contribution. □

Proof of Theorem 2.1. In virtue of Lemma A.1, we can assume that $b(t) = 0$. The following notation is used:

$$h_R(s) := \frac{1}{2R} \mathbf{1}_{[-R,R]}(s), \quad \Gamma_s(t) := \int_{-\infty}^{t} e^{(a+is)u}\sigma(u)\, dW(u),$$

and

$$\sigma_a(t) := e^{at}\sigma(t).$$

Moreover, when not otherwise specified, the integrals are considered on $\mathbb{R}$.

For any fixed s, v, by Itô formula,

$$d(\Gamma_s\overline{\Gamma}_{s+v})(t) = \sigma^2(t)e^{(2a-iv)t}dt + \Gamma_s(t)d\overline{\Gamma}_{s+v}(t) + \overline{\Gamma}_{s+v}(t)d\Gamma_s(t).$$

Therefore

$$\int h_R(s)\mathcal{L}(dp)(a+is)\overline{\mathcal{L}(dp)}(a+is+iv)ds = \int_{-\infty}^{0} \sigma^2(t)e^{(2a-iv)t}dt + \int h_R(s) \int_{-\infty}^{0} \Gamma_s(t)d\overline{\Gamma}_{s+v}(t) + \overline{\Gamma}_{s+v}(t)d\Gamma_s(t)\, ds.$$

We prove that $A_R(v)$, defined by

$$A_R(v) := \int h_R(s) \int_{-\infty}^{0} \Gamma_s(t)d\overline{\Gamma}_{s+v}(t) + \overline{\Gamma}_{s+v}(t)d\Gamma_s(t)\, ds$$

converges to zero in probability as $R \to \infty$. By symmetry it is sufficient to consider

$$A_{R,1}(v) := \int h_R(s) \int_{-\infty}^{0} e^{(a-is-iv)t} \int_{-\infty}^{t} e^{(a+is)u}\sigma(u)\, dW(u)\, \sigma(t)\, dW(t)\, ds.$$

Applying Itô isometry, the Fubini theorem, and the Cauchy–Schwartz inequality yields

$$E[|A_{R,1}(v)|^2] = E[A_{R,1}(v)\overline{A_{R,1}}(v)] = E\Big[\int\int h_R(s)h_R(s')\int_{-\infty}^{0} e^{(2a-i(s-s'))t}\ \Gamma_s(t)\overline{\Gamma_{s'}}(t)\sigma^2(t)\,dt\,ds\,ds'\Big]$$
$$\leq E\Big[\int_{-\infty}^{0}\sigma_a^4(t)\,dt\Big]^{\frac{1}{2}} E\Big[\int_{-\infty}^{0}|\int\int h_R(s)h_R(s')\Gamma_s(t)\overline{\Gamma_{s'}}(t)e^{-i(s-s')t}\,ds\,ds'|^2\,dt\Big]^{\frac{1}{2}}.$$

For any fixed t, consider

$$\int\int h_R(s)h_R(s')\Gamma_s\overline{\Gamma_{s'}}e^{-i(s-s')t}\,ds\,ds',$$

where

$$\Gamma_s := \int_{-\infty}^{0} e^{isy}\widetilde{\sigma}_a(y)dW(y) \quad \text{and} \quad \widetilde{\sigma}_a(y) := \mathbf{1}_{(-\infty,t]}(y)e^{ay}\sigma(y).$$

By the change of variables $u = s - s'$, $w = s$, and using $h_R(w-u) = h_R(u-w)$,

$$\int\int h_R(s)h_R(s')\Gamma_s\overline{\Gamma_{s'}}e^{-i(s-s')t}\,ds\,ds' = \int\int h_R(w)h_R(w-u)\Gamma_w\overline{\Gamma_{w-u}}e^{-iut}\,dw\,du$$
$$= \int (h_R\Gamma * h_R\Gamma)(u)e^{-iut}\,du = \mathcal{F}(h_R\Gamma * h_R\Gamma)(t) = |\mathcal{F}(h_R\Gamma)(t)|^2,$$

where $*$ denotes the convolution product and $\mathcal{F}(g)$ denotes the Fourier transform of a function g. Therefore,

$$E\Big[\Big|\int\int h_R(s)h_R(s')\Gamma_s(t)\overline{\Gamma_{s'}}(t)e^{-i(s-s')t}\,ds\,ds'\Big|^2\Big] = E[|\mathcal{F}(h_R\Gamma)(t)|^4].$$

Observe that

$$\mathcal{F}(h_R\Gamma)(t) = \int h_R(u)\int_{-\infty}^{0} e^{iuy}\widetilde{\sigma}_a(y)dW(y)\ e^{-iut}\,du$$
$$= \int_{-\infty}^{0}\Big(\int h_R(u)e^{iu(y-t)}du\Big)\widetilde{\sigma}_a(y)\,dW(y)$$
$$= \int_{-\infty}^{0}\frac{\sin(R(y-t))}{R(y-t)}\widetilde{\sigma}_a(y)\,dW(y).$$

Therefore, by the Burkholder–Davis–Gundy inequality, it holds that

$$E[|\mathcal{F}(h_R\Gamma)(t)|^4] \leq CE\Big[\int_{-\infty}^{0}\frac{\sin^4(R(y-t))}{(R(y-t))^4}\widetilde{\sigma}_a^4(y)\,dy\Big].$$

Finally, using the change of variables $x = y - t$, $z = t$, one obtains

$$E\Big[\int_{-\infty}^{0}\int_{-\infty}^{0}\frac{\sin^4(R(y-t))}{(R(y-t))^4}\widetilde{\sigma}_a^4(y)\,dy\,dt\Big] \leq E\Big[\int_{-\infty}^{0}\sigma_a^4(y)\,dy\Big]\frac{\pi}{R}.$$

This concludes the proof. □

In the following remark, we write the estimator (8), denoted by $\widehat{\sigma}_a^2(t)$ for ease of notation, in a form which is suitable for the asymptotic analysis.

Remark A.2. Given the discrete time observations $\{t_j\}_{j=0,\dots,n}$, denote $\phi_n(\tau) := \sup\{t_j \in (-\infty, 0] : t_j \leq \tau\}$. Then, the convolution in (3) is equal to

$$\frac{1}{2R}\int_{-R}^{R}\Big(\int_{t_n}^{0}e^{(a+is)\phi_n(\tau)}dp(\tau)\Big)\Big(\int_{t_n}^{0}e^{(a-is-iv)\phi_n(\tau)}dp(\tau)\Big)ds.$$

Applying Itô formula and the inverse Fourier transform, the estimator $\widehat{\sigma}_a^2(t)$ can be written as

$$\int_{t_n}^{0}u_h(t-\phi_n(v))e^{2a\phi_n(v)}\sigma^2(v)dv + \int_{t_n}^{0}u_h(t-\phi_n(v))\int_{t_n}^{v}\varphi(R(\phi_n(v)-\phi_n(u)))e^{a\phi_n(u)}\sigma(u)dW_u\ e^{a\phi_n(v)}\sigma(v)dW_v$$
$$+\int_{t_n}^{0}\int_{t_n}^{v}\varphi(R(\phi_n(v)-\phi_n(u)))u_h(t-\phi_n(u))e^{a\phi_n(u)}\sigma(u)dW_u\ e^{a\phi_n(v)}\sigma(v)dW_v,$$

where u_h is defined by (9) and φ by (10).

Proof of Theorem 3.1. According to Lemma A.1, we can assume that $b = 0$. Therefore, using Remark A.2, for any fixed $t < 0$,

$$\widehat{\sigma}_a^2(t) - \sigma_a^2(t) = \int_{t_n}^0 u_h(t-\phi_n(v))e^{2a\phi_n(v)}\sigma^2(v)dv - \sigma_a^2(t) + A_1(t) + A_2(t),$$

where

$$A_1(t) := \int_{t_n}^0 u_h(t-\phi_n(v_2)) \int_{t_n}^{v_2} \varphi(R(\phi_n(v_2)-\phi_n(v_1))e^{a\phi_n(v_1)}\sigma(v_1)dW_{v_1}e^{a\phi_n(v_2)}\sigma(v_2)dW_{v_2}$$

and

$$A_2(t) := \int_{t_n}^0 \int_{t_n}^{v_2} u_h(t-\phi_n(v_1))\varphi(R(\phi_n(v_2)-\phi_n(v_1))e^{a\phi_n(v_1)}\sigma(v_1)dW_{v_1}e^{a\phi_n(v_2)}\sigma(v_2)dW_{v_2}.$$

First consider

$$\int_{t_n}^0 u_h(t-\phi_n(v))e^{2a\phi_n(v)}\sigma^2(v)dv - \sigma_a^2(t),$$

which can be divided into two terms:

$$\int_{t_n}^0 u_h(t-\phi_n(v))e^{2a\phi_n(v)}\sigma^2(v)dv - \int_{t_n}^0 u_h(t-v)e^{2av}\sigma^2(v)dv \tag{25}$$

$$+ \int_{t_n}^0 u_h(t-v)e^{2av}\sigma^2(v)dv - \sigma_a^2(t). \tag{26}$$

We prove that (25) converges to zero in probability. Formula (25) splits into two terms:

$$\int_{t_n}^0 u_h(t-\phi_n(v))e^{2a\phi_n(v)}\sigma^2(v)dv - \int_{t_n}^0 u_h(t-\phi_n(v))e^{2av}\sigma^2(v)dv \tag{27}$$

$$+ \int_{t_n}^0 u_h(t-\phi_n(v))e^{2av}\sigma^2(v)dv - \int_{t_n}^0 u_h(t-v)e^{2av}\sigma^2(v)dv. \tag{28}$$

First we consider (28). Let $\psi_n(t) := \inf\{t_k \in (-\infty, 0] : t_k \geq t\}$. Then,

$$E\left[\left|\int_{t_n}^0 (u_h(t-\phi_n(v)) - u_h(t-v))\ e^{2av}\sigma^2(v)dv\right|\right]$$

$$\leq E\left[\left|\int_{\psi_n(t-h)}^{\phi_n(t+h)} \sigma_a^2(v)\left(\frac{1}{h}\left(1-\frac{|t-\phi_n(v)|}{h}\right) - \frac{1}{h}\left(1-\frac{|t-v|}{h}\right)\right)dv\right|\right] \tag{29}$$

$$+E\left[\int_{t-h}^{\psi_n(t-h)} \sigma_a^2(v)\frac{1}{h}\left(1-\frac{|t-v|}{h}\right)dv\right] + E\left[\int_{\phi_n(t+h)}^{t+h} \sigma_a^2(v)\frac{1}{h}\left(1-\frac{|t-v|}{h}\right)dv\right]. \tag{30}$$

Consider (29). This is dominated by

$$E\left[\int_{\psi_n(t-h)}^{\phi_n(t+h)} \sigma_a^2(v)\frac{1}{h^2}\ |\phi_n(v)-v|\,dv\right] \leq \frac{\rho(n)}{h}E\left[\frac{1}{h}\int_{\psi_n(t-h)}^{\phi_n(t+h)} \sigma_a^2(v)dv\right] \leq \frac{\rho(n)}{h}E\left[\frac{1}{h}\int_{t-h}^{t+h} \sigma_a^2(v)dv\right] \leq C\frac{\rho(n)}{h}.$$

The last inequality follows from the continuity of the volatility path and assumption (13). A similar argument shows that the two terms appearing in (30) are dominated by $C\frac{\rho(n)}{h}$.

Consider (27), it holds that

$$E\left[\left|\int_{t_n}^0 u_h(t-\phi_n(v))e^{2a\phi_n(v)}\sigma^2(v)dv - \int_{t_n}^0 u_h(t-\phi_n(v))e^{2av}\sigma^2(v)dv\right|\right]$$

$$\leq 2a\rho(n)\int_{t_n}^0 u_h(t-\phi_n(v))\sup_{t_n\leq v\leq 0} E[\sigma_a^2(v)]\ dv \leq C\rho(n)\left(1+\frac{\rho(n)}{h}\right),$$

thanks to hypothesis (13) and the same argument used for (28).

Consider (26). For any $t < 0$ it holds that

$$E\left[\left|\int_{t_n}^{0} u_h(t-v)\sigma_a^2(v)\,dv - \sigma_a^2(t)\right|\right] \le \int_{t-h}^{t+h} \frac{1}{h}\left(1-\frac{|t-v|}{h}\right) E\left[\sup_{\substack{t-h\le v\le t+h\\ v,t\in[t_n,0)}} |\sigma_a^2(v)-\sigma_a^2(t)|\right] dv$$

$$\le E\left[\sup_{\substack{t-h\le v\le t+h\\ v,t\in(-\infty,0)}} |\sigma_a^2(v)-\sigma_a^2(t)|\right].$$

Finally, the last term goes to 0 as $h \to 0$.

We consider now the cross terms $A_1(t)$ and $A_2(t)$. By Itô isometry,

$$E[(A_1(t))^2] = E\left[\int_{t_n}^{0} u_h^2(t-\phi_n(v_2))\left(\int_{t_n}^{v_2} \varphi(R(\phi_n(v_2)-\phi_n(v_1)))e^{a\phi_n(v_1)}dp(v_1)\right)^2 e^{2a\phi_n(v_2)}\sigma^2(v_2)\,dv_2\right]$$

$$\le \int_{t_n}^{0} u_h^2(t-\phi_n(v_2))E\left[\left(\int_{t_n}^{v_2} \varphi(R(\phi_n(v_2)-\phi_n(v_1)))e^{a\phi_n(v_1)}dp(v_1)\right)^4\right]^{\frac{1}{2}} \left(\sup_{t_n\le v_2\le 0} E[e^{4a\phi_n(v_2)}\sigma^4(v_2)]\right)^{\frac{1}{2}} dv_2$$

$$\le C\int_{t_n}^{0} u_h^2(t-\phi_n(v_2))E\left[\left(\int_{t_n}^{v_2} \varphi(R(\phi_n(v_2)-\phi_n(v_1)))e^{a\phi_n(v_1)}dp(v_1)\right)^4\right]^{\frac{1}{2}} dv_2, \tag{31}$$

by the Cauchy–Schwartz inequality and hypothesis (13). Using the Burkholder–Davis–Gundy inequality, the Cauchy–Schwartz inequality, and hypothesis (13), it holds that

$$E\left[\left(\int_{t_n}^{v_2} \varphi(R(\phi_n(v_2)-\phi_n(v_1)))e^{a\phi_n(v_1)}dp(v_1)\right)^4\right]$$

$$\le CE\left[\left(\int_{t_n}^{v_2} \varphi^2(R(\phi_n(v_2)-\phi_n(v_1)))e^{2a\phi_n(v_1)}\sigma^2(v_1)dv_1\right)^2\right]$$

$$\le C\sup_{t_n\le v\le 0} E[e^{4a\phi_n(v)}\sigma^4(v)]\left(\int_{t_n}^{v_2} \varphi^2(R(\phi_n(v_2)-\phi_n(v_1)))dv_1\right)^2$$

$$\le C(\rho(n))^2$$

by Lemma B.1. Finally, (31) converges to 0, being dominated as

$$C\rho(n)\int_{t_n}^{0} u_h^2(t-\phi_n(v_2))dv_2 = C\rho(n) + O\left(\frac{\rho(n)}{h}\right)^2.$$

Finally, the term $A_2(t)$ can be studied in a similar way. This completes the proof. □

Proof of Theorem 3.4. By the continuity of the volatility path, it is not restrictive to suppose that $\operatorname{ess\,sup}\|\sigma^2\|_\infty < C$, where $\|\sigma^2\|_\infty := \sup_{0\le t\le T}|\sigma^2(t)|$. Using the representation in Remark A.2, for any fixed $t < T$ yields

$$\widehat{\sigma}^2(t) = \int_0^T u_h(t-\phi_n(v_2))\sigma^2(v_2)dv_2 + A_1(t) + A_2(t),$$

where

$$A_1(t) := \int_0^T u_h(t-\phi_n(v_2))\int_0^{v_2} \varphi(R(\phi_n(v_2)-\phi_n(v_1))\sigma(v_1)dW_{v_1}\sigma(v_2)dW_{v_2}$$

and

$$A_2(t) := \int_0^T \int_0^{v_2} u_h(t-\phi_n(v_1))\varphi(R(\phi_n(v_2)-\phi_n(v_1))\sigma(v_1)dW_{v_1}\sigma(v_2)dW_{v_2}.$$

We first study the convergence in probability of

$$\sqrt{\frac{nh}{T}}\left(\int_0^T u_h(t-\phi_n(v_2))\,\sigma^2(v_2)dv_2 - \sigma^2(t)\right)$$

$$= \sqrt{\frac{nh}{T}}\left(\int_0^T u_h(t-\phi_n(v_2))\sigma^2(v_2)dv_2 - \int_0^T u_h(t-v_2)\sigma^2(v_2)dv_2\right) \tag{32}$$

$$+\sqrt{\frac{nh}{T}}\left(\int_0^T u_h(t-v_2)\sigma^2(v_2)dv_2-\sigma^2(t)\right). \tag{33}$$

Consider (32). Using the estimation obtained for (28), it holds that

$$\sqrt{\frac{nh}{T}}\left(\int_0^T u_h(t-\phi_n(v_2))\sigma^2(v_2)dv_2-\int_0^T u_h(t-v_2)\sigma^2(v_2)dv_2\right)=O_p((nh)^{-\frac{1}{2}}),$$

so it goes to 0 as $n\to\infty$, $h\to 0$ under the given hypotheses.

Now consider (33). Using (26) and the Lévy modulus of continuity (that is, assumption (H.3)′), we conclude:

$$\sqrt{\frac{nh}{T}}\left(\int_0^T u_h(t-v_2)\sigma^2(v_2)dv_2-\sigma^2(t)\right)=O_p((nh^2|\log(T/h)|)^{\frac{1}{2}}).$$

This goes to 0 as $n\to\infty$, $h\to 0$ under the given hypotheses.

Following Jacod (1997) we now study the asymptotic variance. According to the notation used so far, this means that for any fixed $t\in(0,T)$, we determine the limit in probability of the bracket

$$\langle\sqrt{nh/T}\ (A_1(t)+A_2(t)),\sqrt{nh/T}\ (A_1(t)+A_2(t))\rangle_T. \tag{34}$$

First, consider

$$\langle\sqrt{nh/T}\,A_1(t),\sqrt{nh/T}\,A_1(t)\rangle_T=\frac{nh}{T}\int_0^T u_h^2(t-\phi_n(v_2))\left(\int_0^{v_2}\varphi(R(\phi_n(v_2)-\phi_n(v_1)))\sigma(v_1)dW_{v_1}\right)^2\sigma^2(v_2)dv_2. \tag{35}$$

Applying Itô formula it holds that

$$\left(\int_0^{v_2}\varphi(R(\phi_n(v_2)-\phi_n(v_1)))\sigma(v_1)dW_{v_1}\right)^2=\int_0^{v_2}\varphi^2(R(\phi_n(v_2)-\phi_n(v_1)))\sigma^2(v_1)dv_1$$
$$+2\int_0^{v_2}\left(\int_0^{v_1}\varphi(R(\phi_n(v_2)-\phi_n(u)))\sigma(u)dW_u\right)\varphi(R(\phi_n(v_2)-\phi_n(v_1)))\sigma(v_1)dW_{v_1}.$$

Therefore, in order to study (35), the sum of two terms must be considered:

$$T_1(t):=\int_0^T u_h^2(t-\phi_n(v_2))\int_0^{v_2}\varphi^2(R(\phi_n(v_2)-\phi_n(v_1)))\sigma^2(v_1)dv_1\sigma^2(v_2)dv_2$$

and

$$T_2(t):=2\int_0^T u_h^2(t-\phi_n(v_2))\times\int_0^{v_2}\int_0^{v_1}\varphi(R(\phi_n(v_2)-\phi_n(u)))\sigma(u)dW_u\,\varphi(R(\phi_n(v_2)-\phi_n(v_1)))\sigma(v_1)dW_{v_1}\ \sigma^2(v_2)dv_2.$$

Firstly, we prove that for any $t\in(0,T)$, the following convergence in probability holds:

$$\frac{nh}{T}\ T_1(t)\to\frac{1}{3}(1+2\eta(c))\sigma^4(t). \tag{36}$$

Let $V:=\frac{T}{2}(1+2\eta(c))$. Thus

$$\frac{1}{T}\left|nh\int_0^T u_h^2(t-\phi_n(v_2))\int_0^{v_2}\varphi^2(R(\phi_n(v_2)-\phi_n(v_1)))\sigma^2(v_1)dv_1\ \sigma^2(v_2)dv_2-V\frac{2}{3}\sigma^4(t)\right|$$
$$\le\frac{1}{T}h\int_0^T u_h^2(t-\phi_n(v_2))\left|n\int_0^{v_2}\varphi^2(R(\phi_n(v_2)-\phi_n(v_1)))\sigma^2(v_1)dv_1-V\sigma^2(v_2)\right|\sigma^2(v_2)dv_2 \tag{37}$$
$$+V\frac{1}{T}\left|h\int_0^T u_h^2(t-\phi_n(v_2))\sigma^4(v_2)dv_2-\frac{2}{3}\sigma^4(t)\right|. \tag{38}$$

Consider (37), using the estimation obtained for (28), it holds that

$$\frac{1}{T}h\int_0^T u_h^2(t-v_2)\left|n\int_0^{v_2}\varphi^2(R(\phi_n(v_2)-\phi_n(v_1)))\sigma^2(v_1)dv_1-V\sigma^2(v_2)\right|\sigma^2(v_2)dv_2 \tag{39}$$

converges to 0 in probability. By Lemma B.5 and by Watson and Leadbetter Sankhya (1964), Lemma 3,

$$\left| n \int_0^{\nu_2} \varphi^2(R(\phi_n(\nu_2) - \phi_n(\nu_1)))\sigma^2(\nu_1)d\nu_1 - V\sigma^2(\nu_2) \right| = o_p(1)$$

as $n, R \to \infty$ with $R/n \to c$. As it holds that for any $t \in (0, T)$

$$h \int_0^T u_h^2(t - \nu_2)d\nu_2 = \frac{2}{3}, \tag{40}$$

we conclude that the term (39) is $o_p(1)$.

We now prove that (38) converges to 0 in probability for any $t \in (0, T)$.

Using the same argument as for (28), it is enough to consider

$$\left| h \int_0^T u_h^2(t - \nu_2)\sigma^4(\nu_2)d\nu_2 - \frac{2}{3}\ \sigma^4(t) \right|, \tag{41}$$

which, using (40), is equal to

$$\left| h \int_0^T u_h^2(t - \nu_2)(\sigma^4(\nu_2) - \sigma^4(t))d\nu_2 \right|.$$

Note that because $|t - \nu_2| \leq h$, it follows that:

$$E[|\sigma^4(\nu_2) - \sigma^4(t)|] \leq 2||\sigma^2||_\infty E\left[\sup_{|t-\nu_2|\leq h} |\sigma^2(\nu_2) - \sigma^2(t)| \right] = 2||\sigma^2||_\infty \sqrt{h|\log(T/h)|},$$

thanks to assumption (H.3)′. Therefore, (41) is $O_p(\sqrt{h|\log(T/h)|})$, so by hypothesis, it converges to 0. This completes the proof of (36).

The second step consists in proving that the following convergence in probability holds:

$$\frac{nh}{T}\ T_2(t) \to 0. \tag{42}$$

To this end, with a similar argument as for (28), it is sufficient to show that

$$\int_0^T hu_h^2(t - \nu_2)\ n \int_0^{\nu_2} \left(\int_0^{\nu_1} \varphi(R(\phi_n(\nu_2) - \phi_n(u)))\sigma(u)dW_u \right) \varphi(R(\phi_n(\nu_2) - \phi_n(\nu_1)))\sigma(\nu_1)dW_{\nu_1}\ \sigma^2(\nu_2)d\nu_2 \tag{43}$$

converges to 0 in probability. Consider

$$n \int_0^{\nu_2} \int_0^{\nu_1} \varphi(R(\phi_n(\nu_2) - \phi_n(u)))\sigma(u)dW_u\, \varphi(R(\phi_n(\nu_2) - \phi_n(\nu_1)))\sigma(\nu_1)dW_{\nu_1}.$$

Using Itô isometry, it follows that

$$n^2 E\left[\left(\int_0^{\nu_2} \left(\int_0^{\nu_1} \varphi(R(\phi_n(\nu_2) - \phi_n(u)))\sigma(u)dW_u \right) \varphi(R(\phi_n(\nu_2) - \phi_n(\nu_1)))\sigma(\nu_1)dW_{\nu_1} \right)^2 \right]$$
$$\leq \|\sigma^2\|_\infty^2\ n^2 \int_0^{\nu_2} \int_0^{\nu_1} \varphi^2(R(\phi_n(\nu_2) - \phi_n(u)))du\ \varphi^2(R(\phi_n(\nu_2) - \phi_n(\nu_1)))d\nu_1.$$

Therefore, we have to consider

$$n \int_0^{\nu_2} \left(n \int_0^{\nu_1} \varphi^2(R(\phi_n(\nu_2) - \phi_n(u)))du \right) \varphi^2(R(\phi_n(\nu_2) - \phi_n(\nu_1)))d\nu_1,$$

which is $o(1)$ combining Lemmas B.1 and B.6 (remember that $R = O(n)$; as well, the above term does not depend on h). Finally, for $h \to 0$, we have

$$\int_0^T hu_h^2(t - \nu_2)\sigma^2(\nu_2)d\nu_2 = O_p(1),$$

which concludes the proof of (42).

We now study the term

$$\langle \sqrt{nh/T}\ A_2(t), \sqrt{nh/T}\ A_2(t) \rangle_T = \frac{nh}{T}\ \int_0^T \left(\int_0^{\nu_2} u_h(t - \phi_n(\nu_1))\varphi(R(\phi_n(\nu_2) - \phi_n(\nu_1)))\sigma(\nu_1)dW_{\nu_1} \right)^2 \sigma^2(\nu_2)d\nu_2.$$

Applying Itô's formula, we have to consider the convergence in probability of

$$\frac{nh}{T}\ \widehat{T}_1(t) + \frac{nh}{T}\ \widehat{T}_2(t),$$

where

$$\widehat{T}_1(t) := \int_0^T \int_0^{\nu_2} u_h^2(t-\phi_n(\nu_1))\varphi^2(R(\phi_n(\nu_2)-\phi_n(\nu_1)))\sigma^2(\nu_1)d\nu_1\sigma^2(\nu_2)d\nu_2$$

and

$$\begin{aligned}\widehat{T}_2(t) := 2\int_0^T \int_0^{\nu_2} \left(\int_0^{\nu_1} u_h(t-\phi_n(u))\varphi(R(\phi_n(\nu_2)-\phi_n(u)))\sigma(u)dW_u\right)\\ \times u_h(t-\phi_n(\nu_1))\varphi(R(\phi_n(\nu_2)-\phi_n(\nu_1)))\sigma(\nu_1)dW_{\nu_1}\sigma^2(\nu_2)d\nu_2.\end{aligned}$$

The argument is similar to the case of $A_1(t)$, and we prove the following convergence in probability for any $t \in (0, T)$:

$$\frac{nh}{T}\widehat{T}_1(t) \to \frac{1}{3}(1+2\eta(c))\sigma^4(t)$$

and

$$\frac{nh}{T}\widehat{T}_2(t) \to 0.$$

The other two cross terms contributing to the asymptotic variance are symmetric. Consider

$$\begin{aligned}\langle\sqrt{nh/T}\ A_1(t), \sqrt{nh/T}\ A_2(t)\rangle_T = \frac{nh}{T}\int_0^T u_h(t-\phi_n(\nu_2))\left\{\int_0^{\nu_2}\varphi(R(\phi_n(\nu_2)-\phi_n(\nu_1)))\sigma(\nu_1)dW_{\nu_1}\right\}\\ \times\left\{\int_0^{\nu_2} u_h(t-\phi_n(\nu_1))\varphi(R(\phi_n(\nu_2)-\phi_n(\nu_1)))\sigma(\nu_1)dW_{\nu_1}\right\}\sigma^2(\nu_2)d\nu_2.\end{aligned}$$

Applying Itô's formula to $X(z)Y(z)$, where

$$X(z) = \int_0^z \varphi(R(\phi_n(z)-\phi_n(\nu_1)))\sigma(\nu_1)dW_{\nu_1}$$

and

$$Y(z) = \int_0^z u_h(t-\phi_n(\nu_1))\varphi(R(\phi_n(z)-\phi_n(\nu_1)))\sigma(\nu_1)dW_{\nu_1},$$

we study the convergence in probability of

$$\frac{nh}{T}[\widetilde{T}_1(t) + \widetilde{T}_2(t) + \widetilde{S}_2(t)],$$

where

$$\begin{aligned}\widetilde{T}_1(t) &:= \int_0^T u_h(t-\phi_n(\nu_2))\int_0^{\nu_2} u_h(t-\phi_n(\nu_1))\varphi^2(R(\phi_n(\nu_2)-\phi_n(\nu_1)))\sigma^2(\nu_1)d\nu_1\sigma^2(\nu_2)d\nu_2,\\ \widetilde{T}_2(t) &:= \int_0^T u_h(t-\phi_n(\nu_2))\int_0^{\nu_2}\left(\int_0^{\nu_1} u_h(t-\phi_n(u))\varphi(R(\phi_n(\nu_2)-\phi_n(u)))\sigma(u)dW_u\right)\\ &\quad\times\varphi(R(\phi_n(\nu_2)-\phi_n(\nu_1)))\sigma(\nu_1)dW_{\nu_1}\ \sigma^2(\nu_2)d\nu_2\end{aligned}$$

and

$$\begin{aligned}\widetilde{S}_2(t) := \int_0^T u_h(t-\phi_n(\nu_2))\int_0^{\nu_2}\left(\int_0^{\nu_1}\varphi(R(\phi_n(\nu_2)-\phi_n(u)))\sigma(u)dW_u\right)\\ \times u_h(t-\phi_n(\nu_1))\varphi(R(\phi_n(\nu_2)-\phi_n(\nu_1)))\sigma(\nu_1)dW_{\nu_1}\ \sigma^2(\nu_2)d\nu_2.\end{aligned}$$

We show that in probability

$$\frac{nh}{T}\widetilde{T}_1(t) \to \frac{1}{3}(2\eta(c)+1)\sigma^4(t), \tag{44}$$

$$\frac{nh}{T}\widetilde{T}_2(t) \to 0 \tag{45}$$

and

$$\frac{nh}{T}\widetilde{S}_2(t) \to 0. \tag{46}$$

First consider (44). Let $V := \frac{T}{2}(1+2\eta(c))$. Then

$$\left|\frac{nh}{T}\ \widetilde{T}_1(t) - \frac{1}{T}V\frac{2}{3}\sigma^4(t)\right| \leq \frac{1}{T}|nh\int_0^T u_h(t-\phi_n(v_2))\int_0^{v_2} u_h(t-\phi_n(v_1))\varphi^2(R(\phi_n(v_2)-\phi_n(v_1)))\sigma^2(v_1)dv_1\sigma^2(v_2)\,dv_2$$
$$-Vh\int_0^T u_h^2(t-\phi_n(v_2))\sigma^4(v_2)dv_2| \tag{47}$$

$$+\frac{1}{T}V|h\int_0^T u_h^2(t-\phi_n(v_2))\sigma^4(v_2)dv_2 - \frac{2}{3}\sigma^4(t)|. \tag{48}$$

Consider term (47). For any $h>0$, we define the continuous function

$$\sigma_h^2(r) := u_h(t-r)\sigma^2(r).$$

Using Lemma B.5 and Lemma 3 by Watson and Leadbetter Sankhya (1964), it holds that in probability

$$\lim_{n,R\to\infty} n\int_0^{v_2}\varphi^2(R(\phi_n(v_2)-\phi_n(v_1)))\sigma_h^2(v_1)dv_1 = V\sigma_h^2(v_2).$$

Moreover, observe that (48) is the same as (38). Therefore, the proof follows along the same line with the cross term previously studied. The convergence in probability to 0 of the terms (45) and (46) can be verified through the same arguments as for (42). Finally, considering the four cross terms, we conclude that (34) converges in probability to $\frac{4}{3}(1+2\eta(c))\sigma^4(t)$.

Following Jacod (1997), the last step of the proof requires proving the following convergence in probability:

$$\left\langle\sqrt{\frac{nh}{T}}\,(A_1(t)+A_2(t)), W\right\rangle_T \to 0$$

for any fixed $t\in(0,T)$. We study the details of the convergence of $\langle\sqrt{\frac{nh}{T}}A_1(t), W\rangle_T$; the other term is analogous. To this aim, consider

$$\sqrt{\frac{nh}{T}}\int_0^T u_h(t-\phi_n(v_2))\int_0^{v_2}\varphi(R(\phi_n(v_2)-\phi_n(v_1)))\sigma(v_1)dW_{v_1}\ \sigma(v_2)\,dv_2.$$

We have:

$$\sqrt{\frac{nh}{T}}E\left[\left|\int_0^T u_h(t-\phi_n(v_2))\int_0^{v_2}\varphi(R(\phi_n(v_2)-\phi_n(v_1)))\sigma(v_1)dW_{v_1}\ \sigma(v_2)\,dv_2\right|\right]$$
$$\leq\sqrt{\frac{nh}{T}}\|\sigma\|_\infty\int_0^T u_h(t-\phi_n(v_2))E\left[\left|\int_0^{v_2}\varphi(R(\phi_n(v_2)-\phi_n(v_1)))\sigma(v_1)dW_{v_1}\right|\right]dv_2. \tag{49}$$

Using Itô isometry, it holds that

$$E\left[\left|\int_0^{v_2}\varphi(R(\phi_n(v_2)-\phi_n(v_1)))\sigma(v_1)dW_{v_1}\right|\right] \leq \|\sigma^2\|_\infty^{\frac{1}{2}}\left(\int_0^{v_2}\varphi^2(R(\phi_n(v_2)-\phi_n(v_1)))dv_1\right)^{\frac{1}{2}}.$$

Therefore (49) is dominated by:

$$C\sqrt{h}\int_0^T u_h(t-\phi_n(v_2))\left(n\int_0^{v_2}\varphi^2(R(\phi_n(v_2)-\phi_n(v_1)))dv_1\right)^{\frac{1}{2}}dv_2\,.$$

Observe that

$$\sqrt{h}\int_0^T u_h(t-v_2)\left(n\int_0^{v_2}\varphi^2(R(\phi_n(v_2)-\phi_n(v_1)))dv_1\right)^{\frac{1}{2}}dv_2 \leq C\sqrt{h}\to 0$$

by Lemma B.1 and the identity $\int_0^T u_h(t-v_2)dv_2 = 1$. The conclusion follows an argument similar to (28). This concludes the proof. □

Appendix B. Auxiliary lemmas

Lemma B.1. *For any j, $1\leq j\leq n$, and for $p>1$,*

$$\rho(n)^{-1}\sum_{i=1}^n|\varphi(R(t_i-t_j))|^p(t_i-t_{i-1}) \leq 1+\frac{C_p}{R\rho(n)},$$

where C_p is a suitable constant. Therefore, under the hypothesis that $R\rho(n) \to c_\rho$, $c_\rho \in (0, +\infty)$ as $R \to \infty$ and $\rho(n) \to 0$, it holds that

$$\limsup_n \sup_{t_j} \rho(n)^{-1} \sum_{i=1}^{n} |\varphi(R(t_i - t_j))|^p (t_i - t_{i-1}) \le C_p.$$

Proof. Recall that if $g(x)$: $\mathbf{R} \to \mathbf{R}$ is a positive function, decreasing for $x > 0$ and increasing for $x < 0$, and if $s_0 < s_1 < \ldots < s_n$ is a finite sequence of real numbers such that $s_i - s_{i-1} \le r$ for all i, then

$$\sum_{i=1}^{n} g(s_i)(s_i - s_{i-1}) \le rg(0) + \int_{-\infty}^{+\infty} g(x)dx\,.$$

Consider g as before, integrable, with $g(0) = 1$ and $g \ge |\varphi|^p$ (the inequality holds because $p > 1$). Let $s_i := R(t_i - t_j)$, $r := R\rho(n)$, and $C_p := \int_{-\infty}^{+\infty} g(x)dx$. Then

$$\rho(n)^{-1} \sum_{i=1}^{n} |\varphi(R(t_i - t_j))|^p (t_i - t_{i-1}) = \frac{1}{R\rho(n)} \sum_{i=1}^{n} |\varphi(s_i)|^p (s_i - s_{i-1})$$

$$\le \frac{1}{R\rho(n)} \sum_{i=1}^{n} g(s_i)(s_i - s_{i-1}) \le 1 + \frac{1}{R\rho(n)} \int_{-\infty}^{+\infty} g(x)dx = 1 + \frac{C_p}{R\rho(n)}.$$

□

Lemma B.2. *Let $R/n \to c \in (0, +\infty)$ as $n, R \to +\infty$. It holds that*

$$\sum_{k=1}^{+\infty} \frac{\sin^2(cTk)}{(cTk)^2} = \frac{1}{2\tilde{c}^2} r(\tilde{c})(1 - r(\tilde{c})) =: \eta(c), \tag{50}$$

where $\tilde{c} = c\frac{T}{\pi}$ and $r(z) = z - [z]$, with $[z]$ the integer part of z.

Proof. This follows directly from point (ii) in the proof of Lemma 1 by Clement and Gloter (2011), letting $a := \tilde{c}$. □

Lemma B.3. *Let $R/n \to c \in (0, +\infty)$ as $n, R \to +\infty$, then, for any $s \in (0, T)$, it holds that*

$$\lim_{R,n \to +\infty} n \int_0^{\phi_n(s)+T/n} \varphi^2(R\phi_n(u))du = T(1 + \eta(c)), \tag{51}$$

where $\eta(c)$ is given in (50).

Proof. For $0 < s < T$, let $k_n(s) = n\phi_n(s)/T$. We then have

$$n \int_0^{\phi_n(s)+T/n} \varphi^2(R\phi_n(u))du = T \sum_{k=0}^{k_n(s)} \varphi^2\left(R\frac{T}{n}k\right) = T\left[1 + \sum_{k=1}^{+\infty} \frac{\sin^2(RkT/n)}{(RkT/n)^2} 1_{\{k \le k_n(s)\}}\right] \tag{52}$$

and

$$\lim_{R,n \to +\infty} \frac{\sin^2(RkT/n)}{(RkT/n)^2} = \frac{\sin^2(ckT)}{(ckT)^2}.$$

It is not restrictive to assume that $\frac{R}{n} \ge c$. Therefore

$$\frac{\sin^2(RkT/n)}{(RkT/n)^2} \le \frac{1/T^2}{(ck)^2}, \quad k = 1, 2, \ldots$$

so that from the dominated convergence theorem, we have

$$\lim_{R,n \to +\infty} \sum_{k=0}^{k_n(s)} \varphi^2\left(R\frac{T}{n}k\right) = 1 + \sum_{k=1}^{+\infty} \frac{\sin^2(ckT)}{(ckT)^2}.$$

The limiting result (51) follows using Lemma B.2 and Eq. (52). □

Lemma B.4. *Let the assumptions of Lemma B.3 hold. Then, for any $s \in (0, T)$,*

$$n \int_0^{\phi_n(s)} \varphi^2(R(\phi_n(s) - \phi_n(u)))du = n \int_{T/n}^{\phi_n(s)+T/n} \varphi^2(R\phi_n(v))dv, \tag{53}$$

$$\lim_{R,n \to +\infty} n \int_0^{\phi_n(s)} \varphi^2(R(\phi_n(s) - \phi_n(u)))du = T\eta(c) \tag{54}$$

and

$$\lim_{R,\, n\to+\infty} \int_{\phi_n(s)}^{s} \varphi^2(R(\phi_n(s)-\phi_n(u)))du = \frac{T}{2}. \tag{55}$$

Proof. The two limits (53) and (54) follow using the change of variable $v = \phi_n(s) + \frac{T}{n} - u$, the result (51), and the fact that by continuity, $\varphi(R\phi_n(v)) = 1$ as $v \in (0, T/n)$. We now prove (55). Arguing as in the proof of Lemma 1 (iii) by Clement and Gloter (2011),

$$n\int_{\phi_n(s)}^{s} \varphi^2(R(\phi_n(s)-\phi_n(u)))du = n(s-\phi_n(s)) \tag{56}$$

and

$$\begin{aligned} n\int_{\phi_n(s)}^{s} \varphi^2(R(\phi_n(s)-\phi_n(u)))du &= n\frac{d}{dt}\int_0^t ds \int_{\phi_n(s)}^{s} \varphi^2(R(\phi_n(s)-\phi_n(u)))du \\ &= n\frac{d}{dt}\int_0^t ds(s-\phi_n(s)) = n\frac{d}{dt}\left\{\sum_{k=0}^{k_n(t)-1}\int_{Tk/n}^{T(k+1)/n}(s-k\frac{T}{n})ds + o(1/n)\right\}, \end{aligned} \tag{57}$$

where $k_n(t) = [nt/T]$. Then (55) follows from an easy computation. □

Lemma B.5. *Let the assumptions of Lemma B.3 hold. For any* $s \in (0, T)$,

$$\lim_{R,\, n\to+\infty} n\int_0^s \varphi^2(R(\phi_n(s)-\phi_n(u)))du = \frac{T}{2}(1+2\eta(c)). \tag{58}$$

Proof. Splitting the integral appearing in (58) as

$$n\int_0^{\phi_n(s)} \varphi^2(R(\phi_n(s)-\phi_n(u)))du + n\int_{\phi_n(s)}^{s} \varphi^2(R(\phi_n(s)-\phi_n(u)))du$$

and using Lemma B.4, the thesis follows. □

Lemma B.6. *Let the assumptions of Lemma B.3 hold. Then for any* $v_1, v_2 \in (0, T)$, $v_1 < v_2$,

$$\lim_{R,\, n\to+\infty} \int_0^{v_1} \varphi^2(R(\phi_n(v_2)-\phi_n(u)))du = 0\,. \tag{59}$$

Proof. With the change of variable $q := \phi_n(v_2) - u$, the integral can be rewritten as follows:

$$\int_0^{v_1} \varphi^2(R(\phi_n(v_2)-\phi_n(u)))du = \int_{\phi_n(v_2)-v_1}^{\phi_n(v_2)} \varphi^2(R\phi_n(q)))dq\,.$$

Note that $\phi_n(v_2) - v_1 > 0$ for a large enough n. Setting $k_n(v_1, v_2) := [n(\phi_n(v_2) - v_1)/T]$ and $k_n(v) := n\phi_n(v_2)/T$, we have

$$\begin{aligned} n\int_{\phi_n(v_2)-v_1}^{\phi_n(v_2)} \varphi^2(R\phi_n(q))dq &= n\frac{T}{n}\sum_{k=k_n(v_1,v_2)}^{k_n(v_2)} \varphi^2\left(R\frac{T}{n}k\right) \\ &= T\left[1+\sum_{k=1}^{+\infty}\frac{\sin^2(RkT/n)}{(RkT/n)^2}1_{\{k\le k_n(v_2)\}} - \left(1+\sum_{k=1}^{+\infty}\frac{\sin^2(RkT/n)}{(RkT/n)^2}1_{\{k\le k_n(v_1,v_2)\}}\right)\right] \end{aligned} \tag{60}$$

and

$$\lim_{R,n\to+\infty}\frac{\sin^2(RkT/n)}{(RkT/n)^2} = \frac{\sin^2(ckT)}{(ckT)^2}.$$

It is not restrictive to assume $R/n \ge c$, so

$$\frac{\sin^2(RkT/n)}{(RkT/n)^2}1_{\{k\le k_n(v_2)\}} \le \frac{1/T^2}{(ck)^2}$$

and

$$\frac{\sin^2(RkT/n)}{(RkT/n)^2}1_{\{k\le k_n(v_1,v_2)\}} \le \frac{1/T^2}{(ck)^2}.$$

By the dominated convergence theorem, it follows that

$$\lim_{R,n\to+\infty} \sum_{k=0}^{k_n(v_2)} \varphi^2\left(R\frac{T}{n}k\right) = 1 + \sum_{k=1}^{+\infty} \frac{\sin^2(ckT)}{(ckT)^2}$$

and

$$\lim_{R,n\to+\infty} \sum_{k=0}^{k_n(v_1,v_2)} \varphi^2\left(R\frac{T}{n}k\right) = 1 + \sum_{k=1}^{+\infty} \frac{\sin^2(ckT)}{(ckT)^2}.$$

The limiting result (59) follows using Lemma B.2 and Eq. (60). □

References

Ait-Sahalia, Y., Jacod, J., 2014. High-Frequency Financial Econometrics. Princeton University Press.

Bandi, F. M., & Renò, R. (2010). Nonparametric stochastic volatility. Econometric Theory, forthcoming. Available at SSRN: http://ssrn.com/abstract=1158438.

Bandi, F.M., Russell, J.R., 2006. Separating microstructure noise from volatility. J. Financ. Econ. 79, 655–692.

Barndorff-Nielsen, O.E., Hansen, P.R., Lunde, A., Shephard, N., 2008. Designing realised kernels to measure the ex-post variation of equity prices in the presence of noise. Econometrica 76, 1481–1536.

Barndorff-Nielsen, O.E., Hansen, P.R., Lunde, A., Shephard, N., 2009. Realized kernels in practice: trades and quotes. Econom. J. 12, C1–C32.

Carr, P., Wu, L., 2004. Time-Changed Lévy Processes And Option Pricing. J. Financ. Econ. 71, 113–141.

Clement, E., Gloter, A., 2011. Limit theorems in the Fourier transform method for the estimation of multivariate volatility. Stoch. Process. Appl. 121, 1097–1124.

Cox, J.C., Ingersoll, J.E., Ross, S.A., 1985. A theory of the term structure of interest rates. Econometrica 53, 385–408.

Cuchiero, C., Teichmann, J., 2013. Fourier transform methods for pathwise covariance estimation in the presence of jumps. Stoch. Process. Appl. 125, 116–160.

Fan, J., Wang, Y., 2008. Spot volatility estimation for high frequency data. Stat. Interface 1, 279–288.

Fusai, G., 2004. Pricing Asian options via Fourier and laplace transforms. J. Comput. Financ. 7 (3), 87–106.

Jacod, J., 1997. On continuous conditional Gaussian martingales and stable convergence in law. In: Séminaire de probabilités, XXXI. In: Lecture Notes in Mathematics, 1655. Springer, Berlin, pp. 232–246.

Kanaya, S., Kristensen, D., 2015. Estimation of stochastic volatility models by nonparametric filtering. Econom. Theory 32 (4), 861–916.

Kristensen, D., 2010. Nonparametric filtering of the realized spot volatility: a kernel-based approach. Econom. Theory 26, 60–93.

Leblanc, B., Scaillet, O., 1998. Path dependent options on yields in the affine term structure model. Financ. Stoch. 2, 349–367.

Lee, R.W., 2004. Option pricing by transform methods: extensions, unification and error control. J. Comput. Financ. 7 (3), 51–86.

Malliavin, P., 1995. Integration and Probability. Springer-Verlag.

Malliavin, P., Mancino, M.E., 2002. Fourier series method for measurement of multivariate volatilities. Financ. Stoch. 4, 49–61.

Malliavin, P., Mancino, M.E., 2009. A Fourier transform method for nonparametric estimation of volatility. Ann. Stat. 37 (4), 1983–2010.

Malliavin, P., Mancino, M.E., Barucci, E., 2005. Harmonic analysis methods for nonparametric estimation of volatility: theory and applications. In: Ritsumeikan International Symposium Stochastic Processes and Application to Mathematical Finance. World Scientific Publishing Co., pp. 1–34.

Mancini, C., Mattiussi, V., Renó, R., 2015. Spot volatility estimation using delta sequences. Financ. Stoch. 19, 261–293.

Mancino, M.E., Recchioni, M.C., 2015. Fourier spot volatility estimator: asymptotic normality and efficiency with liquid and illiquid high-frequency data. PLoS One 10 (9), 1–33.

Mancino, M.E., Sanfelici, S., 2008. Robustness of the fourier estimator of integrated volatility in presence of microstructure noise. Comput. Stat. Data Anal. 52 (6), 2966–2989.

Mancino, M.E., Sanfelici, S., 2011. Estimating covariance via fourier method in the presence of asynchronous trading and microstructure noise. J. Financ. Econom. 9 (2), 367–408.

Nielsen, M.O., Frederiksen, P.H., 2008. Finite sample accuracy and choice of sampling frequency in integrated volatility estimation. J. Empir. Financ. 15, 265–286.

Park, S., Linton, O., Hong, S.Y., 2016. Estimating the quadratic covariation matrix for an asynchronously observed continuous time signal masked by additive noise. J. Econom. 191 (2), 325–347.

Tauchen, G., Todorov, V., 2012. The realized Laplace transform of volatility. Econometrica 80, 1105–1127.

Vasicek, O., 1977. An equilibrium characterization of the term structure. J. Financ. Econ. 5 (2), 177–188.

Watson, G.S., Leadbetter Sankhya, M.R., 1964. Hazard analysis II. Indian J. Stat., Ser. A 26 (1), 101–116.